

# Splitting Messages in the Dark— Rate-Splitting Multiple Access for FDD Massive MIMO Without CSI Feedback

Namhyun Kim and Jeonghun Park

**Abstract**—A critical hindrance to realize frequency division duplex (FDD) massive multi-input multi-output (MIMO) systems is overhead associated with downlink channel state information at the transmitter (CSIT) acquisition. To address this challenge, we propose a novel framework that achieves robust performances while completely eliminating downlink CSIT training and feedback. Specifically, by exploiting partial frequency invariance of channel parameters between the uplink (UL) and downlink (DL), we adopt the 2D-Newtonized orthogonal matching pursuit (2D-NOMP) algorithm to reconstruct DL CSIT from UL training. Due to inherent discrepancies arising from a carrier frequency difference between two disjoint bands, however, the multi-user interference is inevitable. To overcome this, we propose a precoding method that employs rate-splitting multiple access (RSMA) and also develop an error covariance matrix (ECM) estimation method by using the observed Fisher information matrix (O-FIM). We find that this ECM estimation is crucial for our precoding design in maximizing the sum spectral efficiency (SE). Simulation results show that our method significantly improves the sum SE compared to other state-of-the-art approaches, underscoring the importance of our ECM estimation.

**Index Terms**—FDD massive MIMO, Error covariance estimation, Rate-splitting multiple access, Generalized power iteration.

## I. INTRODUCTION

Massive multiple-input-multiple-output (MIMO) systems are at the forefront of the future wireless communication paradigm, promising significant gains in spectral efficiency (SE) and reduced cost [1], [2]. To fully unlock the potential of massive MIMO, it is well known that the acquisition of channel state information at the transmitter (CSIT) is key. For this reason, time division duplexing (TDD) has emerged as a predominant approach, thanks to its straightforward channel estimation process that leverages channel reciprocity [1], [3].

Nonetheless, there have been persistent research efforts aimed at realizing the advantages of massive MIMO for frequency division duplexing (FDD) as well [4]–[6]. The enduring importance of these research endeavors is usually underscored by the following considerations. i) The majority of the bandwidth is allocated for the FDD mode in sub-6GHz, which still dominates the cellular market today. Con-

sequently, there is substantial commercial interest in making the FDD massive MIMO systems compatible with existing legacy wireless networks [6], [7]. ii) FDD systems allow simultaneous uplink (UL) and downlink (DL) transmission, catering to delay-sensitive applications [8]. iii) FDD massive MIMO can also offer superior UL coverage compared to TDD, contributing to its cost-effectiveness by potentially reducing CapEx [6], [9]. Despite these benefits, FDD massive MIMO systems encounter significant challenges with the increasing complexity of CSIT acquisition as the number of base station (BS) antennas grows, attributed to their lack of channel reciprocity [5], [10]. In this paper, we take a step towards addressing this challenge.

### A. Prior Work

So far, extensive studies have been conducted to realize FDD massive MIMO systems. We categorize the prior work into two primary approaches: those aimed at reducing CSIT overhead and those aimed at mitigating multi-user interference (MUI).

1) *CSIT overhead reduction approaches*: One of the main principles of these studies is that the DL channel in FDD massive MIMO can be compressed in certain domains. For example, if the compressible domains or bases are known, compressed sensing (CS)-based methods are effective to reduce the amount of CSI training and feedback [11]. For instance, a distributed DL CSIT compression method was developed by [10], which proactively harnesses the shared sparsity structures from local scatterers. In [12], a super-resolution compressed sensing (CS) method was proposed for use in the presence of the beam squint effect in mmWave wideband MIMO-OFDM systems.

Recently, methods not relying on a specific compressible basis but rather on data-driven deep learning have also been actively studied. For example, in [13], CS-ReNet was devised, which jointly exploits deep learning techniques and CS-based compression. Using the universal approximation theorem, the sparse complex-valued neural network (SCNet) was introduced to model the UL/DL relationship in [14]. In [15], it was proposed to use deep learning to map channels from one set of antennas and frequency band to channels of another set, significantly reducing the training overhead. The overview of deep learning based CSIT acquisition was carefully investigated in [16].

N. Kim and J. Park are with the School of Electrical and Electronic Engineering, Yonsei University, Seoul 03722, South Korea. (e-mail: namhyun@yonsei.ac.kr, jhpark@yonsei.ac.kr).

In a different line of research, [17] presented a compelling idea: the DL channel in a FDD mode can be reconstructed by using only UL training, thus eliminating the need for CSI feedback. This approach takes advantages of the frequency-invariant characteristics shared by the UL/DL channels. Specifically, channel parameters such as angle of arrival (AoA) or departure (AoD), delay, and path gains are assumed to be constant between UL/DL channels, given their extrapolation range is not too large. Extensions of this concept were discussed in [4], [18]–[20], with [21] implementing the 2D-Newtonized orthogonal matching pursuit (2D-NOMP) algorithm for DL channel reconstruction, supported by measurement campaigns. However, the accuracy of the reconstructed DL channel is reported to be limited due to discrepancies between UL and DL channels or inaccurate models, as shown in [4] and [19]. This limitation can significantly undermine the SE performance of FDD massive MIMO by increasing the MUI.

2) *MUI mitigation approaches*: In the presence of imperfect CSIT, the major performance degradation is caused by the increasing amount of MUI. To address this issue, MUI mitigation strategies have been explored as another approach to unleash the gains of FDD massive MIMO systems. In [22], an interference alignment type scheme was developed to manage the MUI caused from delayed CSIT. In [23], it was shown that the channels of users in different locations have non-overlapping subspaces within the channel covariance matrices (CCMs), resulting in a natural spatial separation that effectively reduces the MUI.

Recently, an unorthodox type of multiple access, referred as rate-splitting multiple access (RSMA), has been actively explored to handle the MUI [24]. In RSMA, the users partially decode the MUI using successive interference cancellation (SIC), leading to interference decoding gains. This is particularly beneficial when the MUI is strong [25]. The performance gains of RSMA depend heavily on the careful design of linear precoding vectors. However, identifying an optimal precoding structure is not straightforward due to the unique message encoding and decoding conditions inherent in RSMA [24]. To address this, [26] proposed a linear precoder design based on weighted minimum mean square (WMMSE), using the sample average approximation (SAA) technique to take the inaccuracy of CSIT into account. In [27], convexifying the objective function and the decoding constraint of RSMA, a linear precoding design method was developed by exploiting a convex-concave procedure. In addition, a bilinear precoding method has been proposed [28], assuming that the knowledge of CCM is not outdated. [29] considered that the DL channel error covariance can be computed since linear minimum mean square error (LMMSE) is used for DL channel estimation in TDD. Based on this, a generalized power iteration (GPI)-based precoding optimization was proposed.

Notice that the two approaches—CSIT overhead reduction and MUI mitigation—are closely related. Reducing CSIT acquisition resources inevitably leads to less accurate CSIT,

which in turn, negatively affects the signal-to-interference-plus-noise ratio (SINR) due to increased MUI. In this context, to guarantee the robust SE performance while minimizing CSIT acquisition overhead, it is essential to jointly consider an effective MUI mitigation method and a CSIT overhead reduction method. However, most previous studies have focused on one approach while overlooking the other. For instance, [17] proposed the complete elimination of DL channel overhead but did not address how to effectively manage the MUI. Similarly, in [29], an efficient linear precoding scheme for RSMA was developed without considering the reduction of DL channel overhead. This work aims to bridge the gap between these two approaches systematically and explore their synergetic potential.

## B. Contributions

In this paper, we consider a downlink FDD massive MIMO system without CSI feedback. We introduce a channel reconstruction method using the 2D-NOMP algorithm from [21] to extract the key channel parameters such as AoA, delay, and path gain from UL training. Then we reconstruct the DL channel by exploiting the frequency invariance between UL and DL channels. Due to the inherent discrepancies between the UL and DL channels, however, CSIT errors are unavoidable [4], resulting in the MUI. To manage this, we employ group-wise RSMA, which extends conventional RSMA to better suit the channel characteristics of FDD massive MIMO systems. By incorporating the encoding and decoding conditions associated with the group-wise RSMA, we characterize the achievable SE as a function of the precoding vectors, the reconstructed DL channel, and the CSIT error covariance matrix (ECM). Upon this, we formulate a sum SE maximization problem. We summarize our key contributions for addressing this problem as follows.

- **ECM estimation**: In the problem, obtaining the accurate ECM is crucial. However, it is infeasible to directly estimate the ECM in our setup because neither the CSIT distribution nor the true DL channel vector samples are available. To address this issue, we develop a novel ECM estimation method. Our rationale is built on the Cramér-Rao lower bound (CRLB), which provides a lower bound on the mean squared error (MSE) performance of DL channel reconstruction. To compute the CRLB without the CSIT distribution, we employ the observed Fisher information (O-FIM) [30]–[32], which requires only the instantaneously observed signal. The use of O-FIM is justified by its optimal performance in predicting the realized squared error.
- **Precoder optimization**: Harnessing the estimated ECM, we propose a precoder optimization method to maximize the sum SE. The sum SE is not on a tractable form due to the non-smoothness arising from the decoding conditions of group-wise RSMA, and the non-convexity inherent in the sum SE expression. First, to deal with the non-smooth minimum function, we exploit

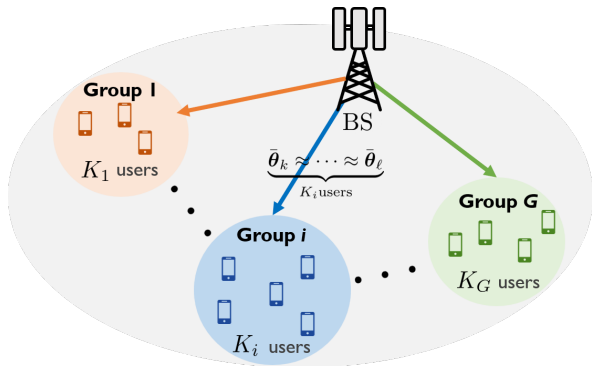


Fig. 1. An illustration of the considered FDD massive MIMO systems. The users are divided into  $G$  groups, and each user in the same group is clustered to have a similar AoA vector  $\bar{\theta}_k$ ,  $k \in [K_i]$ , which is achievable with a high-resolution AoA estimation algorithm.

the LogSumExp technique to approximate the minimum function with a smooth function. Subsequently, we derive the first-order Karush-Kuhn-Tucker (KKT) condition, which can be cast as a form of eigenvector-dependent nonlinear eigenvalue problem (NEPv) [29]. As revealed in [29], in the derived NEPv, the best local optimal solution lies on the leading eigenvector of the NEPv. To find the leading eigenvector, we devise a GPI-based iterative optimization algorithm.

The simulation results reveal important observations as follows. i) Our ECM estimation method based on the O-FIM properly captures the CSIT reconstruction error across the entire extrapolation region. This finding is consistent with those in [30], [31], which showed that the inverse of the O-FIM accurately estimated the realized squared error. ii) The proposed method provides significant improvement in terms of the sum SE compared to the existing method. These gains become more noticeable when the extrapolation model becomes loose. For instance, if mismatched path gains exist, we observe a 5-15% increase in SE at mid-range SNR (10-20dB), and a 41.6% increase at high SNR (40dB). Our method also ensures relatively robust SE performance as the number of paths increases or the extrapolation range expands. iii) Such SE gains cannot be obtained naively; yet, the accurate ECM estimation is crucial. For instance, ignoring the ECM results in up to 32.3% degradation of the sum SE performance, which highlights the critical role of the ECM in achieving the robust SE performance in FDD massive MIMO.

## II. SYSTEM MODEL

We consider a FDD multi-user massive MIMO system, where the BS is equipped with  $N$  antennas and serves  $K$  single-antenna users by sharing the time-frequency resources. We assume that the channel remains time-invariant from the transmission of the UL pilots to the DL precoding [18], [21]. Thus, we are able to reconstruct the DL channel using the information obtained during UL training.

### A. Channel Model

First, we explain our basic assumption regarding the geometric distribution of users. As mentioned in [23], [33], user activity typically occurs within a limited area, allowing for spatial clustering based on user locations. Embracing this, we divide  $K$  users into  $G$  groups as shown in Fig. 1, where group  $i$  includes  $K_i$  users. Within each group, the AoA vectors  $\bar{\theta}_k$ ,  $k \in [K_i]$  are grouped together, based on their similarity. A detailed explanation of a particular clustering method will be provided in Section III.

Next, we introduce the channel model. With orthogonal frequency division multiplexing (OFDM),  $M$  sub-carriers are used for each user in both the DL and UL frequency bands, with sub-carriers spacing of  $\Delta f$ . The total bandwidths of the DL and UL are  $B = M\Delta f$ . Adopting the multipath channel model used in [17], [21], we represent the narrowband UL channel for  $m$ -th sub-carrier of user  $k \in [K]$  as follows

$$\mathbf{h}_k^{\text{ul}}[m] = \sum_{\ell=1}^{L_k^{\text{ul}}} \alpha_{k,\ell}^{\text{ul}} \mathbf{a}(\theta_{k,\ell}^{\text{ul}}; \lambda^{\text{ul}}) e^{-j2\pi m \Delta f \tau_{k,\ell}^{\text{ul}}} \in \mathbb{C}^{N \times 1}, \quad (1)$$

where  $\alpha_{k,\ell}^{\text{ul}}$  is the complex path gain of the  $\ell$ -th path, and  $\mathbf{a}(\theta_{k,\ell}^{\text{ul}}; \lambda^{\text{ul}})$  is the array response defined as

$$\mathbf{a}(\theta_{k,\ell}^{\text{ul}}; \lambda^{\text{ul}}) = \left[ 1, e^{j2\pi \frac{d}{\lambda^{\text{ul}}} \sin \theta_{k,\ell}^{\text{ul}}}, \dots, e^{j2\pi(N-1) \frac{d}{\lambda^{\text{ul}}} \sin \theta_{k,\ell}^{\text{ul}}} \right]^T. \quad (2)$$

Here we denote the AoA as  $\theta_{k,\ell}^{\text{ul}}$ , the wavelength of UL as  $\lambda^{\text{ul}}$ , and the antenna spacing as  $d$  with  $d = \lambda^{\text{ul}}/2$ . Further, we indicate the propagation delay as  $\tau_{k,\ell}^{\text{ul}}$  with  $0 < \tau_{k,\ell}^{\text{ul}} < 1/\Delta f$ , and the number of paths as  $L_k^{\text{ul}}$ . We also assume that the baseband UL signal occupies the interval  $[-B/2, B/2]^1$ . Correspondingly, index  $m$  satisfies  $\lfloor \frac{-M}{2} \rfloor \leq m \leq \lceil \frac{M}{2} \rceil - 1$ ,  $m \in \mathbb{Z}$ .

To model the distribution of the complex path gain  $\alpha_{k,\ell}^{\text{ul}}$ , we use the Rician distribution, i.e.  $\alpha_{k,\ell}^{\text{ul}} \sim \mathcal{CN}\left(\sqrt{\frac{\kappa_k \sigma_{\text{path},k}^2}{\kappa_k + 1}}, \frac{\sigma_{\text{path},k}^2}{\kappa_k + 1}\right)$ . The parameter  $\kappa_k$  denotes the Rician factor of user  $k$  and represents the relative strength of the line-of-sight (LOS) component compared to the non-line-of-sight (NLOS) component. We note that the complex path gains are identical for all sub-carriers within the operating bandwidth [18], [21]. The parameter  $\sigma_{\text{path},k}^2$  denotes the average channel power of each path, i.e.  $\mathbb{E}[|\alpha_{k,\ell}^{\text{ul}}|^2] = \sigma_{\text{path},k}^2$ .

From now on, for notational convenience, we drop the sub-carrier index  $m$ , so that we simply represent  $\mathbf{h}_k^{\text{ul}}[m]$  as  $\mathbf{h}_k^{\text{ul}}$ , and replace  $m\Delta f$  with  $f^{\text{ul}}$ . Accordingly, (1) is rewritten as

$$\mathbf{h}_k^{\text{ul}} = \sum_{\ell=1}^{L_k^{\text{ul}}} \alpha_{k,\ell}^{\text{ul}} \mathbf{a}(\theta_{k,\ell}^{\text{ul}}; \lambda^{\text{ul}}) e^{-j2\pi f^{\text{ul}} \tau_{k,\ell}^{\text{ul}}} \in \mathbb{C}^{N \times 1}. \quad (3)$$

<sup>1</sup>This assumes the convention that the center frequency of the UL band is set to zero, consistent with the frequency of the passband UL carrier.

Based on the UL channel description (3), we also define the DL channel. Assuming that the difference between the UL and DL carrier frequencies is  $f$ , the DL channel is given by

$$\mathbf{h}_k(f) = \sum_{\ell=1}^{L_k^{\text{dl}}} \alpha_{k,\ell}^{\text{dl}} \mathbf{a}(\theta_{k,\ell}^{\text{dl}}; \lambda^{\text{dl}}) e^{-j2\pi f \tau_{k,\ell}^{\text{dl}}} \in \mathbb{C}^{N \times 1}, \quad (4)$$

where  $\alpha_{k,\ell}^{\text{dl}}, \tau_{k,\ell}^{\text{dl}}, \theta_{k,\ell}^{\text{dl}}, \lambda^{\text{dl}}, L_k^{\text{dl}}$  are defined in the equivalent way with the UL channel. Note that  $f$  is also interpreted as an extrapolation range for the DL channel.

As presented in [17], [20] and also supported by actual measurement campaign [4], the UL and DL channels share several frequency invariant parameters. We summarize the frequency invariant parameters as follows.

- Number of channel paths:  $L_k^{\text{ul}} = L_k^{\text{dl}} \triangleq L_k$ .
- AoA (or AoD):  $\theta_{k,\ell}^{\text{ul}} = \theta_{k,\ell}^{\text{dl}}$ .
- Propagation delay:  $\tau_{k,\ell}^{\text{ul}} = \tau_{k,\ell}^{\text{dl}}$ .
- Complex path gain:  $\alpha_{k,\ell}^{\text{ul}} = \alpha_{k,\ell}^{\text{dl}}$ .

We emphasize the critical role of frequency-invariant parameters in reconstructing the DL channel from UL training. However, the assumption of frequency-invariant path gain remains controversial. Although [17], [20] claimed that the complex path gains are also frequency invariant, i.e.  $\alpha_{k,\ell}^{\text{dl}} = \alpha_{k,\ell}^{\text{ul}}$ , the real-world measurement campaign [19], [21] reported that their instantaneous channel gains may differ. Instead, they tend to have a highly correlated second moment. To capture this, instead of considering the exact frequency invariance, we illustrate the DL channel gain by using the first-order Gauss-Markov model:

$$\alpha_{k,\ell}^{\text{dl}} = \eta \alpha_{k,\ell}^{\text{ul}} + \sqrt{1 - \eta^2} g, \quad g \sim \mathcal{CN}(0, \sigma_{\text{path},k}^2), \quad (5)$$

where  $\eta$  is the correlation between the DL and UL channels. For example, if  $\eta = 1$ , our model (5) reduces to the case of perfect reciprocity, while  $\eta = 0$  indicates that UL/DL gains are completely independent. In this sense, our model includes [17], [20] as an edge case.

### B. Signal Model

We consider RSMA, which is a robust multiple access technique against imperfect CSIT [28], [29], [34]. In conventional 1-layer RSMA, each user  $k$ 's message  $W_k$  is split into a common part  $W_{c,k}$  and a private part  $W_{p,k}$ . The common parts of all users' messages and each private part are respectively encoded into a single common stream  $s_c$  and private streams  $s_k, k \in [K]$ . In decoding, each user decodes the common stream first and eliminates it using SIC, while treating all other private streams as noise. Subsequently, the private streams are decoded by treating any remaining interference as noise.

In this paper, we further elaborate the conventional 1-layer RSMA by incorporating the channel characteristics of the considered FDD massive MIMO systems. That is to say, we compose multiple group common streams as in [33]. Suppose that  $G$  user groups are formed and the  $i$ -th group has  $K_i$  users, where  $\sum_{i=1}^G K_i = K$ . We denote a set of the

users included in the  $i$ -th group as  $\mathcal{K}_i$ . Correspondingly, we devise  $G$  number of group common streams, each of which is denoted as  $s_{c,\mathcal{K}_i}$ . The message  $s_{c,\mathcal{K}_i}$  is designed to be decodable to the users in  $\mathcal{K}_i$ , thus we have  $\{W_{c,i}, i \in \mathcal{K}_i\} \rightarrow s_{c,\mathcal{K}_i}$ . The private streams are constructed by following the conventional way. The key idea behind this construction is as follows. The users in the same group tend to have similar spatial channel statistics, leading to the common CCM in the same group [23]. As  $N$  increases, the CCMs in two different groups become nearly orthogonal, preventing the MUI across different groups. For this reason, it is natural to form multiple common streams per group to efficiently mitigate the MUI. In this paper, we refer to this method as group-wise RSMA.

Using group-wise RSMA, the transmit signal is formed by combining the streams and linear precoding vectors, i.e.

$$\mathbf{x} = \sum_{i=1}^G \mathbf{f}_{c,\mathcal{K}_i} s_{c,\mathcal{K}_i} + \sum_{k=1}^K \mathbf{f}_k s_k, \quad (6)$$

where  $\mathbf{f}_{c,\mathcal{K}_i}, \mathbf{f}_k \in \mathbb{C}^N$  are precoding vectors for the common and private stream, respectively. The transmit power constraint is  $\sum_{i=1}^G \|\mathbf{f}_{c,\mathcal{K}_i}\|^2 + \sum_{k=1}^K \|\mathbf{f}_k\|^2 \leq 1$ . At user  $k \in \mathcal{K}_i$ , the received signal is

$$\begin{aligned} r_k = & \mathbf{h}_k(f) \mathbf{f}_{c,\mathcal{K}_i} s_{c,\mathcal{K}_i} + \mathbf{h}_k(f) \mathbf{f}_k s_k \\ & + \sum_{j=1, j \neq i}^G \mathbf{h}_k(f) \mathbf{f}_{c,\mathcal{K}_j} s_{c,\mathcal{K}_j} + \sum_{p=1, p \neq k}^K \mathbf{h}_k(f) \mathbf{f}_p s_p + z_k, \end{aligned} \quad (7)$$

where  $z_k \sim \mathcal{CN}(0, \sigma^2)$  is the additive white Gaussian noise (AWGN).

## III. DOWNLINK CHANNEL RECONSTRUCTION AND PERFORMANCE CHARACTERIZATION

Before going further, we clarify that the BS does not have any knowledge on the DL channel  $\mathbf{h}_k(f)$  in advance. This is a noticeable difference from several prior work [28], [29], [33], which assumed that the long-term DL CCM is given at the BS. Distinguished from this, our work considers that neither the instantaneous CSIT  $\mathbf{h}_k(f)$  nor the long-term DL CCM is available. For this reason, we cannot use any methods relying on long-term DL statistics such as AoD [20]. In this sense, our scenario is not only more practical but also challenging. Under this assumption, we describe the channel reconstruction process and characterize the achievable SE.

### A. Downlink Channel Reconstruction

We represent the UL training signal including all  $M$  sub-carriers simultaneously. Considering the channel model in (4), we define a vector  $\mathbf{u}(\tau, \theta) \in \mathbb{C}^{MN \times 1}$  as

$$[\mathbf{u}(\tau, \theta)]_{[(m'-1)N+1:m'N]} = \mathbf{a}(\theta; \lambda^{\text{ul}}) e^{-j2\pi(\lfloor \frac{M}{2} \rfloor + m' - 1)\Delta f \tau}, \quad (8)$$

where  $1 \leq m' \leq M, m' \in \mathbb{Z}$ . Assuming that all-ones UL sounding reference signal is used, the corresponding UL received signal is given by

$$\mathbf{y}_k = \sum_{\ell=1}^{L_k} \alpha_{k,\ell}^{\text{ul}} \mathbf{u}(\tau_{k,\ell}^{\text{ul}}, \theta_{k,\ell}^{\text{ul}}) + \mathbf{w}_k \in \mathbb{C}^{MN \times 1}, \quad (9)$$

where  $\mathbf{w}_k$  is the AWGN. Note that  $\mathbf{y}_k$  includes the UL training signal received at all the antennas and sub-carriers.

Our aim is to reconstruct the DL channel using (9). To this end, we estimate the three-tuple parameters  $\{\alpha_{k,\ell}^{\text{dl}}, \tau_{k,\ell}^{\text{dl}}, \theta_{k,\ell}^{\text{dl}}\}_{\ell=1, \dots, L_k}$  from  $\mathbf{y}_k$  and rebuild the DL channel by incorporating the frequency invariance. For this purpose, we apply the 2D-NOMP algorithm introduced in [21], [35]. We briefly describe the process of the 2D-NOMP as follows. For a more detailed explanation, one can refer to [21], [35].

For every iteration, the 2D-NOMP algorithm finds the maximum likelihood (ML) estimate of the angle, delay, and channel gain of each path, denoted as  $(\tilde{\alpha}_{k,\ell}, \tilde{\tau}_{k,\ell}, \tilde{\theta}_{k,\ell})$ . With the estimate, the residual signal at the end of the  $i$ -th iteration is computed by

$$\mathbf{y}_r = \mathbf{y}_k - \sum_{\ell=1}^i \tilde{\alpha}_{k,\ell} \mathbf{u}(\tilde{\tau}_{k,\ell}, \tilde{\theta}_{k,\ell}). \quad (10)$$

Note that the initial value of  $\mathbf{y}_r$  is set to  $\mathbf{y}_k$ . In (10), the ML estimation is maximizing

$$f_{y_r}(\alpha_{k,\ell}, \tau_{k,\ell}, \theta_{k,\ell}) \triangleq 2\text{Re}\{\mathbf{y}_r^H \alpha_{k,\ell} \mathbf{u}(\tau_{k,\ell}, \theta_{k,\ell})\} - |\alpha_{k,\ell}|^2 \|\mathbf{u}(\tau_{k,\ell}, \theta_{k,\ell})\|^2. \quad (11)$$

Based on this, three following steps are performed in the  $i$ -th iteration.

1. *New detection*: To maximize (11), the estimates for  $(\tau, \theta)$  are chosen as

$$(\tilde{\tau}, \tilde{\theta}) = \arg \max_{(\tau, \theta) \in \Omega} \frac{|\mathbf{u}^H(\tau, \theta) \mathbf{y}_r|^2}{\|\mathbf{u}(\tau, \theta)\|^2}. \quad (12)$$

With  $(\tilde{\tau}, \tilde{\theta})$ , we obtain the estimate of the channel gain as

$$\tilde{\alpha} = \frac{\mathbf{u}^H(\tilde{\tau}, \tilde{\theta}) \mathbf{y}_r}{\|\mathbf{u}(\tilde{\tau}, \tilde{\theta})\|^2}. \quad (13)$$

2. *Newton refinement*: Now we reduce the off-grid error. To this end, we define the Newton step and the gradient step as

$$\mathbf{n}_{y_r}(\tilde{\alpha}, \tilde{\tau}, \tilde{\theta}) = -\nabla_{(\tau, \theta)}^2 f_{y_r}(\tilde{\alpha}, \tilde{\tau}, \tilde{\theta})^{-1} \nabla_{(\tau, \theta)} f_{y_r}(\tilde{\alpha}, \tilde{\tau}, \tilde{\theta}), \quad (14)$$

$$\mathbf{g}_{y_r}(\tilde{\alpha}, \tilde{\tau}, \tilde{\theta}) = \nabla_{(\tau, \theta)} f_{y_r}(\tilde{\alpha}, \tilde{\tau}, \tilde{\theta}). \quad (15)$$

We then refine  $(\tilde{\tau}, \tilde{\theta})$  obtained in (12) over the continuum via Newton's method [35], i.e.,

$$(\tilde{\tau}, \tilde{\theta}) = (\tilde{\tau}, \tilde{\theta}) + \begin{cases} \mathbf{n}_{y_r}(\tilde{\alpha}, \tilde{\tau}, \tilde{\theta}), & \text{if } \nabla_{(\tau, \theta)}^2 f_{y_r}(\tilde{\alpha}, \tilde{\tau}, \tilde{\theta}) < \mathbf{0} \\ \mu \mathbf{g}_{y_r}(\tilde{\alpha}, \tilde{\tau}, \tilde{\theta}), & \text{else} \end{cases}, \quad (16)$$

where  $\mu$  is the learning rate. After this refinement, the corresponding gain of the  $i$ -th path is recalculated as in (13).

We cyclically repeat this refinement process  $R_c$  times for all the paths found so far.

3. *Update of gains*: In this step, by using the estimates  $(\tilde{\tau}_{k,\ell}, \tilde{\theta}_{k,\ell}), \forall \ell \in [i]$  obtained in the previous step, we lastly calibrate the gains of all the paths with the least square (LS):

$$[\tilde{\alpha}_{k,1}, \tilde{\alpha}_{k,2}, \dots, \tilde{\alpha}_{k,i}] = \tilde{\mathbf{U}}^\dagger \mathbf{y}_k, \quad (17)$$

where  $\tilde{\mathbf{U}} = [\mathbf{u}(\tilde{\tau}_{k,1}, \tilde{\theta}_{k,1}), \mathbf{u}(\tilde{\tau}_{k,2}, \tilde{\theta}_{k,2}), \dots, \mathbf{u}(\tilde{\tau}_{k,i}, \tilde{\theta}_{k,i})]$ .

The algorithm terminates once the stopping criterion, often based on the false alarm rate, is met. We denote the algorithm output as  $\{\hat{\alpha}_{k,\ell}^{\text{ul}}, \hat{\tau}_{k,\ell}^{\text{ul}}, \hat{\theta}_{k,\ell}^{\text{ul}}\}_{\ell=1, \dots, L_k}$ , and let  $\{\hat{\alpha}_{k,\ell}^{\text{dl}}, \hat{\tau}_{k,\ell}^{\text{dl}}, \hat{\theta}_{k,\ell}^{\text{dl}}\}_{\ell=1, \dots, L_k} = \{\eta \hat{\alpha}_{k,\ell}^{\text{ul}}, \hat{\tau}_{k,\ell}^{\text{ul}}, \hat{\theta}_{k,\ell}^{\text{ul}}\}_{\ell=1, \dots, L_k}$  by incorporating the UL/DL frequency invariance property and leveraging the channel gain model in (5).

Finally, we reconstruct the DL channel as

$$\hat{\mathbf{h}}_k(f) = \sum_{\ell=1}^{L_k} \hat{\alpha}_{k,\ell}^{\text{dl}} \mathbf{a}(\hat{\theta}_{k,\ell}^{\text{dl}}, \lambda^{\text{dl}}) e^{-j2\pi f \hat{\tau}_{k,\ell}^{\text{dl}}}. \quad (18)$$

For conciseness, we henceforth denote  $\hat{\mathbf{h}}_k(f)$  as  $\hat{\mathbf{h}}_k$  unless specified otherwise. Before formulating the problem with the estimated channel, we briefly explain user grouping in the following remark.

**Remark 1.** (User grouping in the DL reconstruction) User grouping is important when using our group-wise RSMA. This is because, the BS needs to know that user  $k$  is included in  $\mathcal{K}_i$  to construct  $s_{c, \mathcal{K}_i}$  to be decoded by user  $k$ . Ideally, the user grouping can be done by using the spatial CCMs. However, in our setup, it is not feasible to use such methods because the BS does not know neither the instantaneous CSIT nor the long-term CCMs. To address this issue, we present a useful technique to perform user grouping based on UL training. On the estimated UL channel, we group the channel gain of user  $k$  according to its power, i.e.,

$$\underbrace{|\hat{\alpha}_{k,i}^{\text{ul}}|^2 > |\hat{\alpha}_{k,j}^{\text{ul}}|^2 > \dots > |\hat{\alpha}_{k,\ell}^{\text{ul}}|^2}_{\hat{L}_k}, \quad (19)$$

where  $\hat{\alpha}_{k,i}^{\text{ul}}$  denotes the estimated UL channel gain during the UL training. Then, we find  $\hat{\theta}_k^{\text{ul}} = [\hat{\theta}_{k,i}^{\text{ul}}, \hat{\theta}_{k,j}^{\text{ul}}, \dots, \hat{\theta}_{k,\ell}^{\text{ul}}]^\top$  by following the same order with (19)<sup>2</sup>. With  $\hat{\theta}_k^{\text{ul}}$ , we use an unsupervised clustering algorithm with a fixed number of groups, the most common of which is  $K$ -means clustering [36]. By doing this, we identify virtual user groups that include the users with the similar AoAs.

**B. Spectral Efficiency Characterization and Problem Formulation**

Revisiting the received signal model in (7), we characterize the SE and formulate the main problem of this paper. Since the reconstructed DL channels are available at the BS

<sup>2</sup>Instead of considering all AoAs, one can also predetermine the interested number of AoAs, say  $L$ . For instance, assuming  $L = 1$ , clustering is based only on the AoA of the path with the highest power.

to design the precoding vectors, we write  $\mathbf{h}_k = \hat{\mathbf{h}}_k + \mathbf{e}_k$ , where  $\mathbf{e}_k$  is the DL channel reconstruction error. Treating  $\mathbf{e}_k$  as independent Gaussian noise, the average power of the received signal  $r_k$ ,  $k \in \mathcal{K}_i$  is

$$\begin{aligned} \frac{P_{\text{tot},k}}{P} &\triangleq \frac{\mathbb{E}\{|r_k|^2\}}{P} = \underbrace{|\hat{\mathbf{h}}_k^H \mathbf{f}_{c,\mathcal{K}_i}|^2}_{S_{c,\mathcal{K}_i}} + \underbrace{|\hat{\mathbf{h}}_k^H \mathbf{f}_k|^2}_{S_k} + \underbrace{\sum_{j=1, j \neq i}^G |\hat{\mathbf{h}}_k^H \mathbf{f}_{c,\mathcal{K}_j}|^2}_{I_k} \\ &+ \underbrace{\sum_{p=1, p \neq k}^K |\hat{\mathbf{h}}_k^H \mathbf{f}_p|^2 + \sum_{j=1}^G |\mathbf{e}_k^H \mathbf{f}_{c,\mathcal{K}_j}|^2 + \sum_{p=1}^K |\mathbf{e}_k^H \mathbf{f}_p|^2 + \frac{\sigma^2}{P}}_{I_{c,\mathcal{K}_i}}. \end{aligned} \quad (20)$$

Then we characterize a lower bound on the instantaneous SE of  $s_{c,\mathcal{K}_i}$  at user  $k \in \mathcal{K}_i$  as

$$\begin{aligned} R_{c,\mathcal{K}_i}^{\text{ins.}}(k) &\stackrel{(a)}{\geq} \mathbb{E}_{\{\mathbf{e}_k | \hat{\psi}_k\}} \left[ \log_2 \left( 1 + S_{c,\mathcal{K}_i} I_{c,\mathcal{K}_i}^{-1} \right) \right] \quad (21) \\ &\stackrel{(b)}{\geq} \log_2 \left( 1 + \frac{|\hat{\mathbf{h}}_k^H \mathbf{f}_{c,\mathcal{K}_i}|^2}{\left\{ \sum_{j=1, j \neq i}^G |\hat{\mathbf{h}}_k^H \mathbf{f}_{c,\mathcal{K}_j}|^2 + \mathbf{f}_{c,\mathcal{K}_i}^H \mathbb{E}[\mathbf{e}_k \mathbf{e}_k^H] \mathbf{f}_{c,\mathcal{K}_i} \right.} \right. \\ &\quad \left. \left. + \sum_{p=1}^K |\hat{\mathbf{h}}_k^H \mathbf{f}_p|^2 + \sum_{p=1}^K \mathbf{f}_p^H \mathbb{E}[\mathbf{e}_k \mathbf{e}_k^H] \mathbf{f}_p + \frac{\sigma^2}{P} \right\}} \right) \quad (22) \\ &\stackrel{(c)}{=} \log_2 \left( 1 + \frac{|\hat{\mathbf{h}}_k^H \mathbf{f}_{c,\mathcal{K}_i}|^2}{\left\{ \sum_{j=1, j \neq i}^G |\hat{\mathbf{h}}_k^H \mathbf{f}_{c,\mathcal{K}_j}|^2 + \sum_{p=1}^K |\hat{\mathbf{h}}_k^H \mathbf{f}_p|^2 \right.} \right. \\ &\quad \left. \left. + \sum_{j=1}^G \mathbf{f}_{c,\mathcal{K}_j}^H \mathbf{\Phi}_k \mathbf{f}_{c,\mathcal{K}_j} + \sum_{p=1}^K \mathbf{f}_p^H \mathbf{\Phi}_k \mathbf{f}_p + \frac{\sigma^2}{P} \right\}} \right) \quad (23) \\ &= \bar{R}_{c,\mathcal{K}_i}^{\text{ins.}}(k) \end{aligned}$$

where (a) follows from treating the DL channel reconstruction error as independent Gaussian noise [29], (b) follows Jensen's inequality, and (c) follows from  $\mathbb{E}_{\{\mathbf{e}_k | \hat{\psi}_k\}}[\mathbf{e}_k \mathbf{e}_k^H] = \mathbf{\Phi}_k$ , where we omit the notation of  $\{\mathbf{e}_k | \hat{\psi}_k\}$  due to the space limitation. To guarantee the decodability of  $s_{c,\mathcal{K}_i}$  for the users in  $\mathcal{K}_i$ , the code rate of  $s_{c,\mathcal{K}_i}$  is defined as  $\min_{k \in \mathcal{K}_i} \{\bar{R}_{c,\mathcal{K}_i}^{\text{ins.}}(k)\}$ . Provided that the proper code rate is used, it is guaranteed that  $s_{c,\mathcal{K}_i}$  is successfully decoded and eliminated with SIC. After SIC, we derive a lower bound on the instantaneous SE of  $s_k$  using a similar process:

$$\begin{aligned} R_k^{\text{ins.}} &\geq \mathbb{E}_{\{\mathbf{e}_k | \hat{\psi}_k\}} \left[ \log_2 \left( 1 + S_k I_k^{-1} \right) \right] \quad (24) \\ &\geq \log_2 \left( 1 + \frac{|\hat{\mathbf{h}}_k^H \mathbf{f}_k|^2}{\left\{ \sum_{j=1, j \neq i}^G |\hat{\mathbf{h}}_k^H \mathbf{f}_{c,\mathcal{K}_j}|^2 + \sum_{p=1, p \neq k}^K |\hat{\mathbf{h}}_k^H \mathbf{f}_p|^2 \right.} \right. \\ &\quad \left. \left. + \sum_{j=1, j \neq i}^G \mathbf{f}_{c,\mathcal{K}_j}^H \mathbf{\Phi}_k \mathbf{f}_{c,\mathcal{K}_j} + \sum_{p=1}^K \mathbf{f}_p^H \mathbf{\Phi}_k \mathbf{f}_p + \frac{\sigma^2}{P} \right\}} \right) \quad (25) \\ &= \bar{R}_k^{\text{ins.}} \end{aligned}$$

Now we formulate the sum SE maximization problem. As explained above, to ensure that each user in  $\mathcal{K}_i$  decodes  $s_{c,\mathcal{K}_i}$ , the code rate of  $s_{c,\mathcal{K}_i}$  is set as  $\min_{k \in \mathcal{K}_i} \{\bar{R}_{c,\mathcal{K}_i}^{\text{ins.}}(k)\}$ . Incorporating this, a sum SE maximization problem is given by

$$\mathcal{P}_1 : \quad \underset{\mathbf{f}_{c,\mathcal{K}_1}, \dots, \mathbf{f}_{c,\mathcal{K}_G}, \mathbf{f}_1, \dots, \mathbf{f}_K}{\text{maximize}} \quad \sum_{i=1}^G \min_{k \in \mathcal{K}_i} \{\bar{R}_{c,\mathcal{K}_i}^{\text{ins.}}(k)\} + \sum_{k=1}^K \bar{R}_k^{\text{ins.}} \quad (26)$$

$$\text{subject to} \quad \sum_{i=1}^G \|\mathbf{f}_{c,\mathcal{K}_i}\|^2 + \sum_{k=1}^K \|\mathbf{f}_k\|^2 \leq 1. \quad (27)$$

We note that the global optimum solution of  $\mathcal{P}_1$  is hardly found due to the non-smoothness and non-convexity entailed in the objective function (26). In the next subsection, we present our approach for reformulating (26) into a tractable form.

### C. Problem Reformulation

To approach the solution of our main problem (26), we first transform the objective function (26) into a tractable form. We thus define a high-dimensional precoding vector by stacking all of precoders,  $\mathbf{f}_{c,\mathcal{K}_1}, \dots, \mathbf{f}_{c,\mathcal{K}_G}, \mathbf{f}_1, \dots, \mathbf{f}_K$  as

$$\bar{\mathbf{f}} = [\mathbf{f}_{c,\mathcal{K}_1}^T, \dots, \mathbf{f}_{c,\mathcal{K}_G}^T, \mathbf{f}_1^T, \dots, \mathbf{f}_K^T]^T \in \mathbb{C}^{N(K+G) \times 1}. \quad (28)$$

With  $\bar{\mathbf{f}}$ , we express the SINR of  $s_{c,\mathcal{K}_i}$  as a form of Rayleigh quotient, i.e.  $\bar{\mathbf{f}}^H \mathbf{A}_{c,\mathcal{K}_i}(k) \bar{\mathbf{f}} / \bar{\mathbf{f}}^H \mathbf{B}_{c,\mathcal{K}_i}(k) \bar{\mathbf{f}}$ , where

$$\begin{aligned} \mathbf{A}_{c,\mathcal{K}_i}(k) &= \text{blkdiag}((\hat{\mathbf{h}}_k \hat{\mathbf{h}}_k^H + \mathbf{\Phi}_k), \dots, (\hat{\mathbf{h}}_k \hat{\mathbf{h}}_k^H + \mathbf{\Phi}_k)) \\ &\quad + \mathbf{I}_{N(K+G)} \frac{\sigma^2}{P}, \end{aligned} \quad (29)$$

$$\mathbf{B}_{c,\mathcal{K}_i}(k) = \mathbf{A}_{c,\mathcal{K}_i}(k) - \text{blkdiag}(\mathbf{0}, \dots, \underbrace{\hat{\mathbf{h}}_k \hat{\mathbf{h}}_k^H}_{i\text{-th block}}, \dots, \mathbf{0}). \quad (30)$$

Similar to that, the SINR of  $s_k$  is written as  $\bar{\mathbf{f}}^H \mathbf{A}_k \bar{\mathbf{f}} / \bar{\mathbf{f}}^H \mathbf{B}_k \bar{\mathbf{f}}$ , where

$$\begin{aligned} \mathbf{A}_k &= \text{blkdiag}((\hat{\mathbf{h}}_k \hat{\mathbf{h}}_k^H + \mathbf{\Phi}_k), \dots, \underbrace{\mathbf{0}}_{i\text{-th block}}, \dots, (\hat{\mathbf{h}}_k \hat{\mathbf{h}}_k^H + \mathbf{\Phi}_k)) \\ &\quad + \mathbf{I}_{N(K+G)} \frac{\sigma^2}{P}, \end{aligned} \quad (31)$$

$$\mathbf{B}_k = \mathbf{A}_k - \text{blkdiag}(\mathbf{0}, \dots, \underbrace{\hat{\mathbf{h}}_k \hat{\mathbf{h}}_k^H}_{(G+k)\text{-th block}}, \dots, \mathbf{0}). \quad (32)$$

With this reformulation, we exploit the LogSumExp technique to resolve the non-smoothness involved in (26). Using the LogSumExp technique, we approximate the non-smooth minimum function as

$$\min_{i=1, \dots, N} \{x_i\} \approx -\alpha \log \left( \frac{1}{N} \sum_{i=1}^N \exp \left( \frac{x_i}{-\alpha} \right) \right), \quad (33)$$

where  $\alpha$  determines the accuracy of the approximation. As  $\alpha \rightarrow 0$ , the approximation becomes tight. For conciseness, we represent

$$g(\{x_i\}_{i \in [N]}) = -\alpha \log \left( \frac{1}{N} \sum_{i=1}^N \exp \left( \frac{x_i}{-\alpha} \right) \right). \quad (34)$$

Leveraging (33), we approximate the SE of  $s_{c, \mathcal{K}_i}$  as

$$\min_{k \in \mathcal{K}_i} \{\bar{R}_{c, \mathcal{K}_i}^{\text{ins.}}(k)\} \approx g \left( \left\{ \frac{\bar{\mathbf{f}}^H \mathbf{A}_{c, \mathcal{K}_i}(k) \bar{\mathbf{f}}}{\bar{\mathbf{f}}^H \mathbf{B}_{c, \mathcal{K}_i}(k) \bar{\mathbf{f}}} \right\}_{k \in \mathcal{K}_i} \right). \quad (35)$$

Using this, we reformulate the original problem  $\mathcal{P}_1$  defined in (26) as

$$\mathcal{P}_2 : \underset{\bar{\mathbf{f}}}{\text{maximize}} \sum_{i=1}^G g \left( \left\{ \frac{\bar{\mathbf{f}}^H \mathbf{A}_{c, \mathcal{K}_i}(k) \bar{\mathbf{f}}}{\bar{\mathbf{f}}^H \mathbf{B}_{c, \mathcal{K}_i}(k) \bar{\mathbf{f}}} \right\}_{k \in \mathcal{K}_i} \right) + \sum_{k=1}^K \log_2 \left( \frac{\bar{\mathbf{f}}^H \mathbf{A}_k \bar{\mathbf{f}}}{\bar{\mathbf{f}}^H \mathbf{B}_k \bar{\mathbf{f}}} \right). \quad (36)$$

In  $\mathcal{P}_2$ , we drop the constraint (27) since the objective function of  $\mathcal{P}_2$  is scale invariant. Note that this does not hurt the optimality as presented in [29]. Even with this reformulation, however, it is still infeasible to solve  $\mathcal{P}_2$ . The main reason is that the ECM  $\Phi_k$ ,  $k \in [K]$  cannot be computed at the BS. In the next section, we explain the challenges in detail and put forth our idea for estimating the ECM.

#### IV. ERROR COVARIANCE MATRIX ESTIMATION

One critical hindrance to solve  $\mathcal{P}_2$  in (36) is that the BS cannot obtain the exact ECM defined as  $\mathbb{E}_{\mathbf{e}_k | \hat{\psi}_k} [\mathbf{e}_k \mathbf{e}_k^H] = \Phi_k$ . To understand the difficulty, we first summarize the conventional approaches to obtain an ECM. For simplicity, we let  $L_k = 1$ ,  $\kappa_k = 0$ , and  $\sigma_{\text{path}, k}^2 = 1$  in the following explanation.

- **Bayesian approach:** In this approach, we directly calculate the ECM by using given DL channel statistics. Assuming that the AoD, denoted as  $\theta_k^{\text{dl}}$ , is known at the BS and it only varies slowly, we obtain the CCM  $\mathbb{E}[\mathbf{h}_k \mathbf{h}_k^H] = \mathbf{a}(\theta_k^{\text{dl}}; \lambda^{\text{dl}}) \cdot \mathbf{a}(\theta_k^{\text{dl}}, \lambda^{\text{dl}})^H = \mathbf{R}_k$ . If the BS applies linear MMSE to estimate the DL channel based on pilot signals, the ECM is given as

$$\hat{\Phi}_k = \mathbf{R}_k - \mathbf{R}_k \left( \mathbf{R}_k + \sigma_{\text{pilot}}^2 \mathbf{I}_N \right)^{-1} \mathbf{R}_k, \quad (37)$$

where  $\sigma_{\text{pilot}}^2$  is the SNR of the pilot signals [29].

- **Frequentist approach:** In this case, instead of using the channel statistics, we assume that multiple numbers of the error samples are available. For instance, denoting the  $i$ -th DL channel error sample as  $\mathbf{e}_k(i)$  with  $i \in [T]$ , the sample ECM is obtained as

$$\hat{\Phi}_k = \frac{1}{T} \sum_{i=1}^T \mathbf{e}_k(i) \mathbf{e}_k^H(i) + \rho \mathbf{I}, \quad (38)$$

where  $\rho$  is a regularization parameter induced to establish well-conditioned  $\hat{\Phi}_k$  [37].

Unfortunately, neither approach is available in our case. First, we assume that no long-term DL channel statistics (including the statistics of the AoD  $\theta_{k, \ell}^{\text{dl}}$ ) are given at the BS in our scenario. Further, it is difficult to analyze the ECM by using 2D-NOMP due to its non-linearity. Additionally, the true DL channel vectors are not known at the BS, thus the sample ECM cannot be obtained.

To address this challenge, we give our attention to the 2D-NOMP algorithm's near-CRLB MSE performance as shown in [35]. This result implies that the ECM can be tightly estimated by leveraging the CRLB [18], whose trace gives a lower bound on the MSE for an unbiased estimator. Considering the relationship between the UL and DL channels and assuming reciprocal path gain in (5) (i.e.  $\eta = 1$ ) for now, we derive the CRLB by using the Jacobian transformation [38], which is given by

$$\Phi_k \succeq (\mathbf{J}_k(f))^H \mathbf{I}^{-1}(\psi_k) \mathbf{J}_k(f) = \mathbf{C}(f), \quad (39)$$

where  $\psi_k$  is the true UL channel parameters defined as

$$\psi_k = (\bar{\psi}_{k,1}^T, \dots, \bar{\psi}_{k,\ell}^T)^T \in \mathbb{R}^{4L_k \times 1}, \quad (40)$$

$$\bar{\psi}_{k,\ell} = (\theta_{k,\ell}^{\text{ul}}, \tau_{k,\ell}^{\text{ul}}, \text{Re}\{\alpha_{k,\ell}^{\text{ul}}\}, \text{Im}\{\alpha_{k,\ell}^{\text{ul}}\})^T \in \mathbb{R}^{4 \times 1}. \quad (41)$$

Further,  $\mathbf{J}_k(f) \in \mathbb{C}^{4L_k \times N}$  denotes the Jacobian matrix evaluated at the extrapolation range  $f$  and  $\mathbf{I}(\psi_k) \in \mathbb{C}^{4L_k \times 4L_k}$  indicates the FIM of user  $k$ . Specifically, the Jacobian matrix  $\mathbf{J}_k(f)$  is defined as

$$\mathbf{J}_k(f) \triangleq \frac{\partial \mathbf{h}_k^T(f)}{\partial \psi_k}, \quad (42)$$

where  $\mathbf{h}_k^T(f)$  is (4).

An implication in (39) is that  $[\Phi_k]_{n,n} \geq [\mathbf{C}(f)]_{n,n}, \forall n$ . Notably, considering the near-optimal MSE performance of 2D-NOMP, we estimate the diagonal component of the ECM by using the CRLB while ignoring the off-diagonal components, i.e.

$$\hat{\Phi}_k \simeq \mathbf{C}(f) \circ \mathbf{I}_N. \quad (43)$$

To use (43) as the estimated ECM, however, we note that the FIM  $\mathbf{I}(\psi_k)$  should be evaluated on the true UL channel parameter  $\psi_k$ , which is typically not available in practice [30]. One maybe tempted to use the estimated parameter  $\hat{\psi}_k$  to calculate (43), yet this compromises the interpretation of the FIM. To address this, we propose to use the O-FIM [31]. The relation of the O-FIM to the FIM and the derivation of the O-FIM are provided in the following remark and lemma, respectively.

**Remark 2** (O-FIM and FIM). Fundamentally, the FIM is derived as

$$\mathbf{I}(\psi_k) = \mathbb{E} \left[ - \frac{\partial^2 \log f(\mathbf{y} | \psi_k)}{\partial \psi_k \partial \psi_k^T} \right], \quad (44)$$

where the expectation is taken with respect to the observation  $\mathbf{y}$  conditioned on the true parameter  $\psi_k$ . On the contrary, the O-FIM is defined as an instantaneous observation of the FIM. This observed information can be interpreted as a sampled version of (44), given by

$$\tilde{\mathbf{I}}(\hat{\psi}_k) = - \frac{\partial^2 \log f(\mathbf{y} | \psi_k)}{\partial \psi_k \partial \psi_k^T} \Bigg|_{\psi_k = \hat{\psi}_k}, \quad (45)$$

which is computable easily with the estimated parameters.

**Lemma 1.** Assuming that the likelihood for the observed signal  $\mathbf{y}$  follows the Gaussian distribution, each element of the O-FIM in (45), calculated only with the UL estimated parameter,  $\hat{\psi}_k$ , is

$$[\tilde{\mathbf{I}}(\hat{\psi}_k)]_{u,v} = \frac{2}{\sigma^2} \text{Re} \left\{ \sum_{n=1}^N \sum_{m=1}^M \left( \frac{\partial \bar{\mathbf{y}}_{n,m}^*}{\partial \psi_u} \frac{\partial \bar{\mathbf{y}}_{n,m}}{\partial \psi_v} \right) - \sum_{n=1}^N \sum_{m=1}^M (\mathbf{y}_{n,m} - \bar{\mathbf{y}}_{n,m})^* \frac{\partial^2 \bar{\mathbf{y}}_{n,m}}{\partial \psi_u \partial \psi_v} \right\} \Big|_{\psi_k = \hat{\psi}_k}, \quad (46)$$

where  $\bar{\mathbf{y}}(\psi_k)$  the reconstructed UL channel with the parameter set  $\psi_k$ , defined as

$$\bar{\mathbf{y}}(\psi_k) \triangleq \sum_{\ell=1}^{L_k} \alpha_{k,\ell}^{\text{ul}} \mathbf{u}(\tau_{k,\ell}^{\text{ul}}, \theta_{k,\ell}^{\text{ul}}) \in \mathbb{C}^{MN \times 1}. \quad (47)$$

*Proof.* See Appendix A.  $\square$

We find an interesting observation on the O-FIM in [30], [31], which showed that the O-FIM is optimal in estimating the realized squared error. Extending it into our case, we get

$$\begin{aligned} & (\tilde{\mathbf{J}}_k(f))^{\text{H}} \tilde{\mathbf{I}}^{-1}(\hat{\psi}_k) \tilde{\mathbf{J}}_k(f) \\ &= \arg \min_{\hat{\Phi}_k} \mathbb{E}_{\mathbf{e}_k | \hat{\psi}_k} \left[ \sum_{m=1}^N \left[ \mathbf{e}_k \mathbf{e}_k^{\text{H}} - \hat{\Phi}_k \right]_{m,m}^2 \right], \end{aligned} \quad (48)$$

where  $\tilde{\mathbf{J}}(f) = \frac{\partial \hat{\mathbf{h}}_k^{\text{T}}(f)}{\partial \hat{\psi}_k} \in \mathbb{C}^{4L_k \times N}$  and  $\tilde{\mathbf{I}}(\hat{\psi}_k)$  is obtained in Lemma 1. Using Jensen's inequality on the right-hand side of (48) and omitting the notation  $\mathbf{e}_k | \hat{\psi}_k$ , we obtain,

$$\sum_{m=1}^N \left[ \mathbb{E} \left[ \mathbf{e}_k \mathbf{e}_k^{\text{H}} \right] - \hat{\Phi}_k \right]_{m,m}^2 \leq \mathbb{E} \left[ \sum_{m=1}^N \left[ \mathbf{e}_k \mathbf{e}_k^{\text{H}} - \hat{\Phi}_k \right]_{m,m}^2 \right]. \quad (50)$$

Notice that the solution derived from (48) actually minimizes an upper bound of the MSE associated with the diagonal elements of the ECM estimation as shown in (50). This provides strong support of using the O-FIM to estimate the ECM. With this, the estimated ECM is given in the following proposition.

**Proposition 1.** The estimated ECM, which minimizes the upper bound of the MSE for its diagonal elements, is derived using the O-FIM as follows

$$\hat{\Phi}_k \triangleq \left( (\tilde{\mathbf{J}}(f))^{\text{H}} \tilde{\mathbf{I}}^{-1}(\hat{\psi}_k) \tilde{\mathbf{J}}(f) \right) \circ \mathbf{I}_N = \tilde{\mathbf{C}}(f). \quad (51)$$

We note that  $\hat{\Phi}_k$  in Proposition 1 can be calculated solely by the estimated UL channel parameter  $\hat{\psi}_k$ , which is valuable in practical scenarios. It is worth to mention that  $\hat{\Phi}_k$  in Proposition 1 assumes the reciprocal path gain, i.e.,  $\eta = 1$ . It is needed to further calibrate the estimated ECM incorporating a case that  $\eta < 1$  as shown in the following corollary.

**Corollary 1.** Taking  $\eta$  into account, the estimated ECM is modified to

$$\hat{\Phi}_k \triangleq \eta^2 \tilde{\mathbf{C}}(f) + L_k (1 - \eta^2) \sigma_{\text{path},k}^2 \mathbf{I}_N, \quad (52)$$

where  $\tilde{\mathbf{C}}(f)$  is given by (51).

*Proof.* See Appendix B.  $\square$

We remark that our ECM estimation depends only on diagonal component as in (51) since its intuition is based on the proposed estimator's near-CRLB performance. However, in Section VI, we will show that this approach is still very useful, especially for a case where the DL channel reconstruction errors are not negligible. Using  $\hat{\Phi}_k$  in (52), we eventually reach  $\mathcal{P}_3$  as follows:

$$\mathcal{P}_3 : \underset{\bar{\mathbf{f}}}{\text{maximize}} \sum_{i=1}^G g \left( \left\{ \frac{\bar{\mathbf{f}}^{\text{H}} \hat{\mathbf{A}}_{c,\mathcal{K}_i}(k) \bar{\mathbf{f}}}{\bar{\mathbf{f}}^{\text{H}} \hat{\mathbf{B}}_{c,\mathcal{K}_i}(k) \bar{\mathbf{f}}} \right\}_{k \in \mathcal{K}_i} \right) + \sum_{k=1}^K \log_2 \left( \frac{\bar{\mathbf{f}}^{\text{H}} \hat{\mathbf{A}}_k \bar{\mathbf{f}}}{\bar{\mathbf{f}}^{\text{H}} \hat{\mathbf{B}}_k \bar{\mathbf{f}}} \right), \quad (53)$$

where we define  $\hat{\mathbf{A}}_{c,\mathcal{K}_i}(k)$ ,  $\hat{\mathbf{B}}_{c,\mathcal{K}_i}(k)$ ,  $\hat{\mathbf{A}}_k$ , and  $\hat{\mathbf{B}}_k$  by replacing every occurrence of  $\Phi_k$  in (29)-(32) with  $\hat{\Phi}_k$ . We note that each element in (53) can be configured based on the information obtained from the UL training. Now we are ready to develop an algorithm to solve (53).

**Remark 3** (ECM estimation in a precoder design aspect). The ECM is important to devise a robust precoder. As observed in (23) and (25), the ECM is incorporated into the interference term of the SINR. This allows the precoder  $\bar{\mathbf{f}}$  to account for the impact of CSIT errors in an average sense. This intuition is theoretically supported in [20]. In [20], it was shown that the outer product of the DL channel ( $\mathbf{h}_k(f) \mathbf{h}_k(f)^{\text{H}}$ ) is identical to the outer product of the estimated DL channel added by the ECM ( $\hat{\mathbf{h}}_k \hat{\mathbf{h}}_k^{\text{H}} + \Phi_k$ ), provided that  $N \rightarrow \infty$ . As a result, accurately estimating the ECM ( $\hat{\Phi}_k \simeq \Phi_k$ ) and incorporating it into the precoder design is essential in achieving the robust SE performance. In Section VI, we validate this intuition by showing that, even with the same precoding method, the robust SE is achievable only with our ECM estimation.

## V. PRECODER OPTIMIZATION

In this section, we propose a precoding optimization method to solve the problem (53). Following the GPI-based precoding method, our method is built by harnessing the following first-order optimality condition.

**Theorem 1.** For problem (53), the first-order optimality condition is satisfied when the following holds:

$$\mathbf{B}_{\text{KKT}}^{-1}(\bar{\mathbf{f}}) \mathbf{A}_{\text{KKT}}(\bar{\mathbf{f}}) \bar{\mathbf{f}} = \lambda(\bar{\mathbf{f}}) \bar{\mathbf{f}}, \quad (57)$$

where each matrix is shown at the bottom of the page.

*Proof.* See Appendix C.  $\square$

As well explained in [29], (57) is interpreted as a form of NEPv. Specifically, the matrix  $\mathbf{B}_{\text{KKT}}^{-1}(\bar{\mathbf{f}}) \mathbf{A}_{\text{KKT}}(\bar{\mathbf{f}})$  is a nonlinear matrix function of  $\bar{\mathbf{f}}$ , and its eigenvalue  $\lambda(\bar{\mathbf{f}})$  is equivalent to the objective function of our main problem (53). Further, the first-order optimality condition is fulfilled



when (57) holds. For this reason, if we find an eigenvector  $\bar{\mathbf{f}}$  that satisfies (57), we can reach a stationary point of (53) whose gradient is zero; yet its optimality cannot be guaranteed due to the non-convexity of (53). Crucially, if we find the leading eigenvector of (57), denoted as  $\bar{\mathbf{f}}^*$ , it maximizes our objective function of (53), and also makes the gradient as zero. To obtain  $\bar{\mathbf{f}}^*$ , we exploit the GPI-based approach.

Given  $(t - 1)$ th iteration, we construct the matrices  $\mathbf{A}_{\text{KKT}}$ ,  $\mathbf{B}_{\text{KKT}}$  as specified in (54) and (55). Then, we calculate the precoding vector for each iteration as

$$\bar{\mathbf{f}}_{(t)} \leftarrow \frac{\mathbf{B}_{\text{KKT}}^{-1}(\bar{\mathbf{f}}_{(t-1)})\mathbf{A}_{\text{KKT}}(\bar{\mathbf{f}}_{(t-1)})\bar{\mathbf{f}}_{(t-1)}}{\|\mathbf{B}_{\text{KKT}}^{-1}(\bar{\mathbf{f}}_{(t-1)})\mathbf{A}_{\text{KKT}}(\bar{\mathbf{f}}_{(t-1)})\bar{\mathbf{f}}_{(t-1)}\|}. \quad (58)$$

Note that this process is repeated until the update of precoder is bounded by predefined parameter, which is  $\|\bar{\mathbf{f}}_{(t)} - \bar{\mathbf{f}}_{(t-1)}\| < \epsilon$ .

## VI. SIMULATION RESULTS

In this section, we first investigate the MSE performance of 2D-NOMP in the DL channel reconstruction to justify our ECM estimation. Then, we demonstrate the ergodic sum SE performance of the proposed method by comparing to the other baseline methods.

### A. MSE of DL Channel Reconstruction

We examine the MSE performance of the 2D-NOMP algorithm in the DL channel reconstruction. The MSE of the estimated DL channel of user  $k$ , i.e.  $\hat{\mathbf{h}}_k(f)$ , is defined as

$$\text{MSE} = \mathbb{E} \left[ \|\mathbf{h}_k(f) - \hat{\mathbf{h}}_k(f)\|^2 \right]. \quad (59)$$

The detailed simulation parameters are described in the caption of Fig. 2.

In Fig. 2, we illustrate the actual MSE (59) of the 2D-NOMP algorithm per extrapolation range  $f$ . We also compare the analytical MSE obtained by the CRLB and by our ECM estimation in (51). To yield the MSE from the CRLB and the estimated ECM, we compute  $\frac{1}{N}\text{tr}(\mathbf{C}(f))$

and  $\frac{1}{N}\text{tr}(\hat{\Phi}_k)$ , where we follow the approach in [18] to compute the  $\mathbf{C}(f)$ . First, we see that the actual MSE of 2D-NOMP is close to the CRLB. This indicates that 2D-NOMP achieves the near-optimal MSE performance in the DL channel reconstruction, which is consistent with [35]. More importantly, we also observe that the actual MSE is more tightly tracked by our ECM estimation. It is evident that the O-FIM reflects the actual MSE more accurately than the theoretical CRLB, aligning with the findings in [32]. This result justifies the use of the O-FIM for the ECM estimation, not only because of its practical applicability but also due to its accuracy.

### B. Ergodic Sum Spectral Efficiency

Now we examine the ergodic sum SE of the proposed method in the context of FDD massive MIMO without CSI feedback. In the simulations, we generate the channel environments by following the channel model in Section II. The detailed simulation parameters are specified in the caption of Fig. 3. As baseline methods, we consider the followings.

- **GPI**: As a state-of-art precoding design method, we consider GPI proposed in [39].
- **WMMSE**: As another state-of-art precoding optimization, we consider WMMSE [40].
- **MRT**: The precoders are aligned by the estimated channel vector, i.e.  $\mathbf{f}_k = \hat{\mathbf{h}}_k$ ,  $k \in \mathcal{K}$ .
- **RZF**: The precoders are designed as

$$\mathbf{f}_k = \left( \hat{\mathbf{H}}\hat{\mathbf{H}}^H + \mathbf{I} \frac{\sigma^2}{P} \right)^{-1} \hat{\mathbf{h}}_k^H, \quad (60)$$

where  $\hat{\mathbf{H}}$  denotes the matrix formed by stacking all the users' estimated channels.

In Fig. 3, we show the ergodic sum SE for the proposed method and the baseline methods, assuming  $\eta^2 = 1$  (upper of Fig. 3) and  $\eta^2 = 0.9$  (lower of Fig. 3). For a case without  $\hat{\Phi}$ , we assume  $\hat{\Phi} = \mathbf{0}$ . First, we see that the proposed method provides significant SE gains over GPI and WMMSE, especially at mid-range or higher SNRs. In particular, the relative performance gap between the proposed and existing

$$\mathbf{A}_{\text{KKT}}(\bar{\mathbf{f}}) = \lambda_{\text{num}}(\bar{\mathbf{f}}) \times \left[ \sum_{k=1}^K \frac{\hat{\mathbf{A}}_k}{\bar{\mathbf{f}}^H \hat{\mathbf{A}}_k \bar{\mathbf{f}}} + \sum_{i=1}^G \left\{ \sum_{k \in \mathcal{K}_i} \left( \frac{\exp\left(\frac{1}{-\alpha} \frac{\bar{\mathbf{f}}^H \hat{\mathbf{A}}_{c, \mathcal{K}_i}(k) \bar{\mathbf{f}}}{\bar{\mathbf{f}}^H \hat{\mathbf{B}}_{c, \mathcal{K}_i}(k) \bar{\mathbf{f}}}\right)}{\sum_{j \in \mathcal{K}_i} \exp\left(\frac{1}{-\alpha} \log_2 \left( \frac{\bar{\mathbf{f}}^H \hat{\mathbf{A}}_{c, \mathcal{K}_i}(j) \bar{\mathbf{f}}}{\bar{\mathbf{f}}^H \hat{\mathbf{B}}_{c, \mathcal{K}_i}(j) \bar{\mathbf{f}}}\right)} \right)}{\bar{\mathbf{f}}^H \hat{\mathbf{A}}_{c, \mathcal{K}_i}(k) \bar{\mathbf{f}}} \right\} \right] \quad (54)$$

$$\mathbf{B}_{\text{KKT}}(\bar{\mathbf{f}}) = \lambda_{\text{den}}(\bar{\mathbf{f}}) \times \left[ \sum_{k=1}^K \frac{\hat{\mathbf{B}}_k}{\bar{\mathbf{f}}^H \hat{\mathbf{B}}_k \bar{\mathbf{f}}} + \sum_{i=1}^G \left\{ \sum_{k \in \mathcal{K}_i} \left( \frac{\exp\left(\frac{1}{-\alpha} \frac{\bar{\mathbf{f}}^H \hat{\mathbf{A}}_{c, \mathcal{K}_i}(k) \bar{\mathbf{f}}}{\bar{\mathbf{f}}^H \hat{\mathbf{B}}_{c, \mathcal{K}_i}(k) \bar{\mathbf{f}}}\right)}{\sum_{j \in \mathcal{K}_i} \exp\left(\frac{1}{-\alpha} \log_2 \left( \frac{\bar{\mathbf{f}}^H \hat{\mathbf{A}}_{c, \mathcal{K}_i}(j) \bar{\mathbf{f}}}{\bar{\mathbf{f}}^H \hat{\mathbf{B}}_{c, \mathcal{K}_i}(j) \bar{\mathbf{f}}}\right)} \right)}{\bar{\mathbf{f}}^H \hat{\mathbf{B}}_{c, \mathcal{K}_i}(k) \bar{\mathbf{f}}} \right\} \right] \quad (55)$$

$$\lambda(\bar{\mathbf{f}}) = \prod_{k=1}^K \left( \frac{\bar{\mathbf{f}}^H \hat{\mathbf{A}}_k \bar{\mathbf{f}}}{\bar{\mathbf{f}}^H \hat{\mathbf{B}}_k \bar{\mathbf{f}}} \right) \times \prod_{i=1}^G \left\{ \frac{1}{K_i} \sum_{k \in \mathcal{K}_i} \exp\left( \log_2 \left( \frac{\bar{\mathbf{f}}^H \hat{\mathbf{A}}_{c, \mathcal{K}_i}(k) \bar{\mathbf{f}}}{\bar{\mathbf{f}}^H \hat{\mathbf{B}}_{c, \mathcal{K}_i}(k) \bar{\mathbf{f}}} \right) \right)^{-\frac{1}{\alpha}} \right\}^{-\frac{\alpha}{\log_2 e}} = \frac{\lambda_{\text{num}}(\bar{\mathbf{f}})}{\lambda_{\text{den}}(\bar{\mathbf{f}})} \quad (56)$$

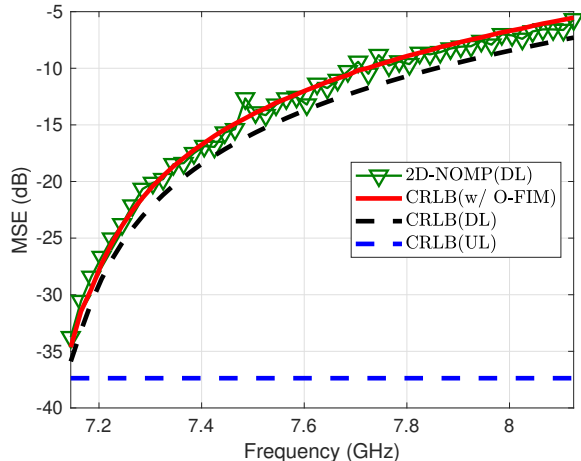


Fig. 2. MSE over DL extrapolation range. The UL carrier frequency is 7.15 GHz and the UL SNR is assumed to be 10dB and  $M = 128$ .

methods is larger when the path gain reciprocity does not hold ( $\eta \neq 1$ ). To be specific, the performance gains over GPI are identified as 5-15% in the mid-range (10-20dB) and up to 41.6% at 40dB. These gains come from that RSMA effectively manages the MUI, which is caused from the imperfect DL channel reconstruction, leading to the robust SE performance thanks to SIC. It is also important to note that the ECM plays a critical role in achieving the robust SE. For example, at SNR 40dB in Fig. 3, neglecting the ECM causes 32.3% degradation in terms of the sum SE, which implies that realizing full potential gains of RSMA requires a delicate treatment of the CSIT error. As explained in Remark 3, the ECM allows the precoder to reflect the impact of CSIT errors into its design, so that we obtain the SIC gains more effectively. Through simulations, we arrive at the following conclusions: the proposed method offers considerable performance gains by leveraging RSMA, and our ECM estimation is key to extract the gains of RSMA.

### C. Robustness in No CSI-Feedback

Now we investigate the robustness of the proposed method. In Fig. 4, we describe the ergodic sum SE of the proposed method per number of paths. We compare three cases: (i) WMMSE [40] with perfect CSIT, (ii) GPI [39] with the DL channel reconstruction, and (iii) the proposed method. Remarkably, for the single-path scenario ( $L_{\{k \in [K]\}} = L = 1$ ), both the GPI precoding with 2D-NOMP DL channel reconstruction and the proposed method achieve the sum SE similar to that under perfect CSIT. This indicates that when  $L = 1$ , the DL channel reconstruction is done with near perfect accuracy. However, as the number of paths increases, the DL channel parameters to be estimated in 2D-NOMP also increase, leading to less accurate DL channel reconstruction. In this case, the proposed method offers robustness. For instance, the proposed method provides 88.6% of performance gains over GPI in 15 paths and 16

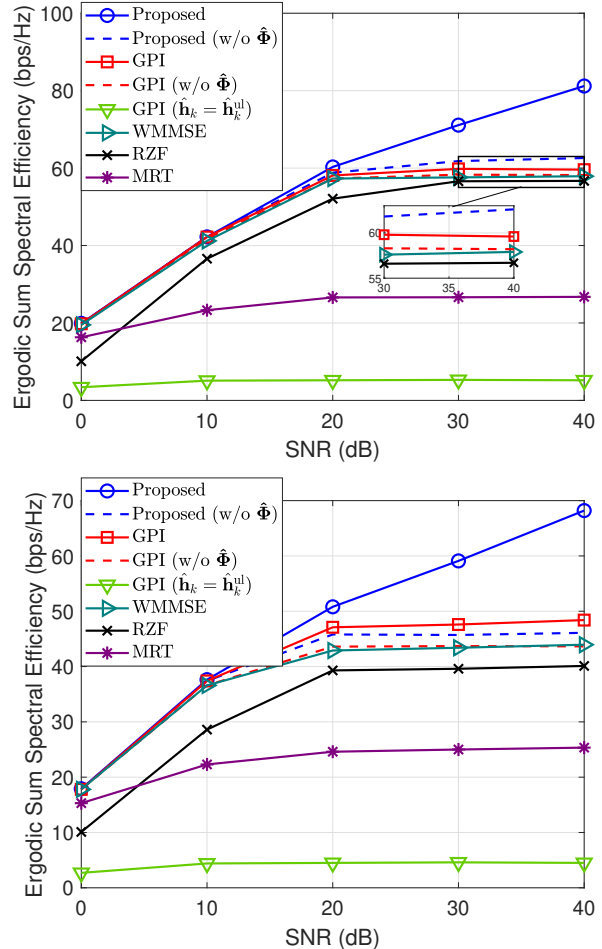


Fig. 3. Comparison of the ergodic sum SE over SNR with  $(N, K) = (32, 16)$  and  $M = 128$ . The UL carrier frequency is 7.15GHz, and the DL carrier frequency is 7.865GHz, which is 10% higher than UL. We assume  $\eta^2 = 1$  (upper) and  $\eta^2 = 0.9$  (lower) and  $G = 4$  for both cases. For the proposed precoding method, we use  $\epsilon = 0.1$  and  $\alpha = 0.1$ .

antennas, which means that our method is powerful when inaccurate DL channel estimation is unavoidable.

Fig. 5 shows the sum SE per extrapolation range  $f$ , assuming the UL frequency of 7.15 GHz. First, we observe that even applying the DL reconstruction technique, it is inevitable to have the SE degradation proportional to  $f$ . In such cases, the proposed method is useful to obtain the robust SE. Specifically, while the performance of GPI and the proposed method are similar when the frequency difference between DL and UL is small, the sum SE performance of the proposed method steadily outperforms that of GPI as the frequency gap increases. Additionally, it is confirmed that if the UL channel is used as the DL channel without proper reconstruction, meaningful SE cannot be obtained even with a small frequency difference. We also find that if the extrapolation range is too large, supplementary DL channel information (e.g. path gain feedback in [21]) might be useful to obtain additional performance improvement.

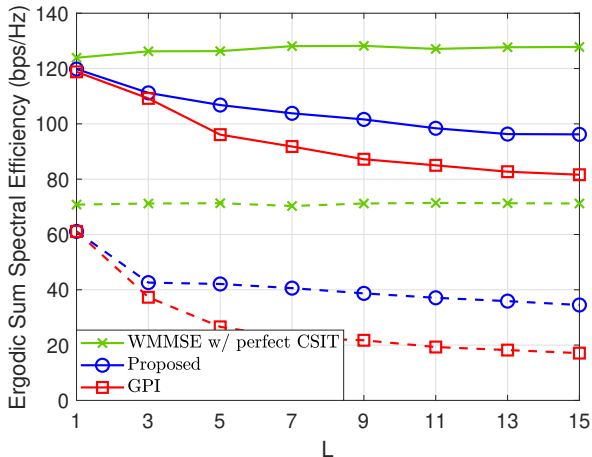


Fig. 4. The ergodic sum SE per number of paths ( $L_{\{k \in [K]\}} = L$ ). The solid line represents  $(N, K) = (64, 32)$  and the dashed line indicates  $(N, K) = (16, 8)$ . SNR = 20dB. Other simulation settings are identical to Fig. 3.

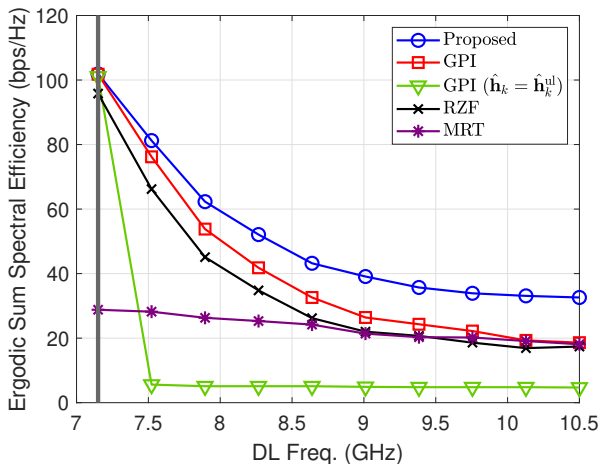


Fig. 5. Comparison of the ergodic sum SE over extrapolation range with  $(N, K) = (32, 16)$ . The UL carrier frequency is fixed at 7.15GHz and  $L_k = 5$ .

## VII. CONCLUSIONS

In this paper, we proposed a novel method to provide the robust SE performance in FDD massive MIMO systems without relying on CSI feedback. The key idea of the proposed method is reconstructing the DL channel based on the UL training by leveraging the frequency invariant properties of key channel parameters. Due the UL/DL discrepancy, however, it is infeasible to perfectly estimate the DL channel from the UL training, which incurs the MUI. To efficiently handle the MUI, our method exploits group-wise RSMA, by which SIC gains are achieved in the presence of MUI. Achieving SIC gains requires to incorporate the CSIT error into precoder design in a delicate way, wherein the proposed ECM estimation is essential. Our major findings are as follows. i) The proposed ECM estimation using the O-FIM accurately captures DL CSIT reconstruction errors. ii) The

proposed method significantly enhances the sum SE performance over the existing methods, particularly noticeable at mid to high SNRs. The gains become pronounced when the DL CSIT reconstruction errors increase, e.g., when path gains between DL and UL are mismatched. iii) Accurate ECM estimation is crucial for achieving the benefits of SIC.

As future work, it is possible to extend our framework by considering various system environments, such as energy efficiency, max-min fairness, and integrated sensing and communications.

## APPENDIX A

### PROOF OF LEMMA 1

Let us assume each measurement  $\mathbf{y}_{n,m}$  at each antenna and sub-carrier ( $n \in [N], m \in [M]$ ) is drawn under independent and identically distributed with likelihood  $f(\mathbf{y}_{n,m}|\psi_k)$ , and its distribution follows a (circularly symmetric complex) Gaussian distribution with covariance  $\sigma^2 \mathbf{I}$  and mean  $\bar{\mathbf{y}}$ . Then, the log-likelihood of the parameters  $\psi_k$  given measured signal can be represented by

$$\mathcal{L}(\psi_k | \mathbf{y}_{n,m}, n \in [N], m \in [M]) \triangleq \sum_{n=1}^N \sum_{m=1}^M \log f(\mathbf{y}_{n,m} | \psi_k) \quad (61)$$

$$= -\frac{1}{\sigma^2} (\mathbf{y} - \bar{\mathbf{y}})^H (\mathbf{y} - \bar{\mathbf{y}}) + C, \quad (62)$$

where  $C$  is a constant. Then, the observed information defined as the negative of the second derivative of log-likelihood is evaluated at instantaneous channel parameters  $\hat{\psi}_k$  as follows [31]

$$\mathbf{I}(\hat{\psi}_k) = -\nabla \nabla^H \mathcal{L}(\psi_k) |_{\psi_k = \hat{\psi}_k} \quad (63)$$

$$= - \begin{bmatrix} \frac{\partial^2}{\partial \psi_{1,1}^2} & \frac{\partial^2}{\partial \psi_{1,1} \partial \psi_{1,2}} & \cdots & \frac{\partial^2}{\partial \psi_{1,1} \partial \psi_{L,4}} \\ \frac{\partial^2}{\partial \psi_{1,2} \partial \psi_{1,1}} & \frac{\partial^2}{\partial \psi_{1,2}^2} & \cdots & \frac{\partial^2}{\partial \psi_{1,2} \partial \psi_{L,4}} \\ \vdots & \vdots & \ddots & \vdots \\ \frac{\partial^2}{\partial \psi_{L,4} \partial \psi_{1,1}} & \frac{\partial^2}{\partial \psi_{L,4} \partial \psi_{1,2}} & \cdots & \frac{\partial^2}{\partial \psi_{L,4}^2} \end{bmatrix} \mathcal{L}(\psi_k) \Big|_{\psi_k = \hat{\psi}_k}, \quad (64)$$

where  $\mathcal{L}(\psi_k)$  denotes  $\mathcal{L}(\psi_k | \mathbf{y}_{n,m}, n \in [N], m \in [M])$  for simplicity and  $\mathcal{L}(\psi_k) |_{\psi_k = \hat{\psi}_k}$  follows the normal distribution as well. To evaluate  $(u, v)$  component of  $\mathbf{I}(\hat{\psi}_k)$ , we compute

$$\begin{aligned} \frac{\partial \mathcal{L}(\psi_k)}{\partial \psi_v} &= \frac{1}{\sigma^2} \sum_{n=1}^N \sum_{m=1}^M \left( \frac{\partial \bar{\mathbf{y}}_{n,m}}{\partial \psi_v} \right)^* (\mathbf{y}_{n,m} - \bar{\mathbf{y}}_{n,m}) \\ &\quad + \frac{1}{\sigma^2} \sum_{n=1}^N \sum_{m=1}^M (\mathbf{y}_{n,m} - \bar{\mathbf{y}}_{n,m})^* \left( \frac{\partial \bar{\mathbf{y}}_{n,m}}{\partial \psi_v} \right), \\ &= \frac{2}{\sigma^2} \text{Re} \left\{ \sum_{n=1}^N \sum_{m=1}^M (\mathbf{y}_{n,m} - \bar{\mathbf{y}}_{n,m})^* \left( \frac{\partial \bar{\mathbf{y}}_{n,m}}{\partial \psi_v} \right) \right\}, \end{aligned}$$

and its derivative with respect to  $\psi_u$  can be found as follows

$$\frac{\partial}{\partial \psi_u} \left( \frac{\partial \mathcal{L}(\psi_k)}{\partial \psi_v} \right) = \frac{2}{\sigma^2} \text{Re} \left\{ \sum_{n=1}^N \sum_{m=1}^M \left( -\frac{\partial \bar{y}_{n,m}^*}{\partial \psi_u} \frac{\partial \bar{y}_{n,m}}{\partial \psi_v} \right) \right. \\ \left. + \sum_{n=1}^N \sum_{m=1}^M (y_{n,m} - \bar{y}_{n,m})^* \frac{\partial^2 \bar{y}_{n,m}}{\partial \psi_u \partial \psi_v} \right\}. \quad (65)$$

$$(66)$$

Substituting (65) into (64) completes the proof.

## APPENDIX B

### PROOF OF COROLLARY 1

We initially characterize the original ECM of the reconstructed DL channel for user  $k$ , denoted as  $\Phi_k$ . This is under the assumption of perfect reciprocity of channel gain, meaning that  $\alpha_k = \alpha_k^{\text{ul}} = \alpha_k^{\text{dl}} \in \mathbb{C}^{L_k \times 1}$ . It can be represented as follows

$$\mathbb{E}[(\mathbf{U}_k \alpha_k - \hat{\mathbf{U}}_k \hat{\alpha}_k)(\mathbf{U}_k \alpha_k - \hat{\mathbf{U}}_k \hat{\alpha}_k)^H], \quad (67)$$

where each column of  $\mathbf{U}_k \in \mathbb{C}^{N \times L_k}$  is given by  $\mathbf{a}(\theta_{k,\ell}^{\text{dl}}, \lambda^{\text{dl}}) e^{-j2\pi f \tau_{k,\ell}^{\text{dl}}} \in \mathbb{C}^{N \times 1}$ .

Subsequently, we will compare (67) with the case in which true DL path gain  $\alpha_k^{\text{dl}}$  is updated by (5), and its MMSE estimator is given with  $\hat{\alpha}^{\text{dl}} = \eta \hat{\alpha}^{\text{ul}}$ . Then, corresponding (true) DL ECM with the Gaussian innovation term  $\mathbf{g} \in \mathbb{C}^{L_k \times 1}$  is,

$$\Phi_k^{\text{new}}(f) = \mathbb{E}[(\mathbf{U}_k \alpha_k^{\text{dl}} - \hat{\mathbf{U}}_k \hat{\alpha}_k^{\text{dl}})(\mathbf{U}_k \alpha_k^{\text{dl}} - \hat{\mathbf{U}}_k \hat{\alpha}_k^{\text{dl}})^H] \quad (68)$$

$$= \mathbb{E}[\mathbf{U}_k (\eta \alpha_k^{\text{ul}} + \sqrt{1 - \eta^2} \mathbf{g}) - \eta \hat{\mathbf{U}}_k \hat{\alpha}_k^{\text{ul}} \\ \times \mathbf{U}_k (\eta \alpha_k^{\text{ul}} + \sqrt{1 - \eta^2} \mathbf{g}) - \eta \hat{\mathbf{U}}_k \hat{\alpha}_k^{\text{ul}})^H]. \quad (69)$$

By manipulating (69), it can be further developed as follows

$$\Phi_k^{\text{new}}(f) = \mathbb{E}[(\eta(\mathbf{U}_k \alpha_k^{\text{ul}} - \hat{\mathbf{U}}_k \hat{\alpha}_k^{\text{ul}}) + \sqrt{1 - \eta^2} \mathbf{U}_k \mathbf{g}) \\ \times (\eta(\mathbf{U}_k \alpha_k^{\text{ul}} - \hat{\mathbf{U}}_k \hat{\alpha}_k^{\text{ul}}) + \sqrt{1 - \eta^2} \mathbf{U}_k \mathbf{g})^H] \quad (70)$$

$$= \mathbb{E}[\eta^2 (\mathbf{U}_k \alpha_k^{\text{ul}} - \hat{\mathbf{U}}_k \hat{\alpha}_k^{\text{ul}})(\mathbf{U}_k \alpha_k^{\text{ul}} - \hat{\mathbf{U}}_k \hat{\alpha}_k^{\text{ul}})^H \\ + (1 - \eta^2) \mathbf{U}_k \mathbb{E}[\mathbf{g} \mathbf{g}^H] \mathbf{U}_k^H] \quad (71)$$

$$= \eta^2 \Phi_k(f) + (1 - \eta^2) \sigma_{\text{path},k}^2 \mathbf{U}_k \mathbf{I}_{L \times L} \mathbf{U}_k^H \quad (72)$$

$$= \eta^2 \Phi_k(f) + L_k (1 - \eta^2) \sigma_{\text{path},k}^2 \mathbf{I}_n, \quad (73)$$

where  $\Phi_k(f)$  is the true ECM with  $\eta = 1$ . Note that (71) follows from the assumption: the error that occurs in UL training with 2D-NOMP is uncorrelated with the Gaussian innovation term, i.e.  $\mathbb{E}[(\mathbf{U}_k \alpha_k^{\text{ul}} - \hat{\mathbf{U}}_k \hat{\alpha}_k^{\text{ul}}) \mathbf{g}^H] = 0$ . Finally, the estimation of  $\Phi_k^{\text{new}}(f)$  is obtained by substituting (51) for  $\Phi_k(f)$  in (73), which completes the proof.

## APPENDIX C

### PROOF OF THEOREM 1

We first explore the KKT condition of our main problem (53). In this, we develop the Lagrangian function as

$$L(\bar{\mathbf{f}}) = \sum_{i=1}^G \log \left( \frac{1}{K_i} \sum_{k \in \mathcal{K}_i} \exp \left( \log_2 \left( \frac{\bar{\mathbf{f}}^H \mathbf{A}_{c,\mathcal{K}_i}(k) \bar{\mathbf{f}}}{\bar{\mathbf{f}}^H \mathbf{B}_{c,\mathcal{K}_i}(k) \bar{\mathbf{f}}} \right) \right)^{-\frac{1}{\alpha}} \right)^{-\alpha} \\ + \sum_{k=1}^K \log_2 \left( \frac{\bar{\mathbf{f}}^H \mathbf{A}_k \bar{\mathbf{f}}}{\bar{\mathbf{f}}^H \mathbf{B}_k \bar{\mathbf{f}}} \right). \quad (74)$$

Then, we take the partial derivatives of  $L(\bar{\mathbf{f}})$  in terms of  $\bar{\mathbf{f}}$  to find a stationary point, where we set it as zero. For notational simplicity, we denote the first term of (74) as  $L_1(\bar{\mathbf{f}})$  and second term as  $L_2(\bar{\mathbf{f}})$  respectively, and each partial derivative is obtained respectively, as follows

$$\frac{\partial L_1(\bar{\mathbf{f}})}{\partial \bar{\mathbf{f}}^H} = \sum_{i=1}^G \left\{ \sum_{k \in \mathcal{K}_i} \left( \frac{\exp \left( \frac{1}{-\alpha} \frac{\bar{\mathbf{f}}^H \mathbf{A}_{c,\mathcal{K}_i}(k) \bar{\mathbf{f}}}{\bar{\mathbf{f}}^H \mathbf{B}_{c,\mathcal{K}_i}(k) \bar{\mathbf{f}}} \right)}{\sum_{j \in \mathcal{K}_i} \exp \left( \frac{1}{-\alpha} \log_2 \left( \frac{\bar{\mathbf{f}}^H \mathbf{A}_{c,\mathcal{K}_i}(j) \bar{\mathbf{f}}}{\bar{\mathbf{f}}^H \mathbf{B}_{c,\mathcal{K}_i}(j) \bar{\mathbf{f}}} \right) \right)} \right) \right\} \\ \times \partial \left( \log_2 \left( \frac{\bar{\mathbf{f}}^H \mathbf{A}_{c,\mathcal{K}_i}(k) \bar{\mathbf{f}}}{\bar{\mathbf{f}}^H \mathbf{B}_{c,\mathcal{K}_i}(k) \bar{\mathbf{f}}} \right) \right) / \partial \bar{\mathbf{f}}^H \quad (75)$$

$$= \frac{1}{\log 2} \sum_{i=1}^G \left\{ \sum_{k \in \mathcal{K}_i} \left( \frac{\exp \left( \frac{1}{-\alpha} \frac{\bar{\mathbf{f}}^H \mathbf{A}_{c,\mathcal{K}_i}(k) \bar{\mathbf{f}}}{\bar{\mathbf{f}}^H \mathbf{B}_{c,\mathcal{K}_i}(k) \bar{\mathbf{f}}} \right)}{\sum_{j \in \mathcal{K}_i} \exp \left( \frac{1}{-\alpha} \log_2 \left( \frac{\bar{\mathbf{f}}^H \mathbf{A}_{c,\mathcal{K}_i}(j) \bar{\mathbf{f}}}{\bar{\mathbf{f}}^H \mathbf{B}_{c,\mathcal{K}_i}(j) \bar{\mathbf{f}}} \right) \right)} \right) \right\} \\ \times \left[ \frac{\mathbf{A}_{c,\mathcal{K}_i}(k) \bar{\mathbf{f}}}{\bar{\mathbf{f}}^H \mathbf{A}_{c,\mathcal{K}_i}(k) \bar{\mathbf{f}}} - \frac{\mathbf{B}_{c,\mathcal{K}_i}(k) \bar{\mathbf{f}}}{\bar{\mathbf{f}}^H \mathbf{B}_{c,\mathcal{K}_i}(k) \bar{\mathbf{f}}} \right], \quad (76)$$

$$\frac{\partial L_2(\bar{\mathbf{f}})}{\partial \bar{\mathbf{f}}^H} = \frac{1}{\log 2} \sum_{k=1}^K \left[ \frac{\mathbf{A}_k \bar{\mathbf{f}}}{\bar{\mathbf{f}}^H \mathbf{A}_k \bar{\mathbf{f}}} - \frac{\mathbf{B}_k \bar{\mathbf{f}}}{\bar{\mathbf{f}}^H \mathbf{B}_k \bar{\mathbf{f}}} \right]. \quad (77)$$

It is obvious that when the sum of both terms is zero, stationarity for first-order KKT condition is met, which is

$$\frac{\partial L_1(\bar{\mathbf{f}})}{\partial \bar{\mathbf{f}}^H} + \frac{\partial L_2(\bar{\mathbf{f}})}{\partial \bar{\mathbf{f}}^H} = 0 \quad (78)$$

$$\Leftrightarrow \sum_{i=1}^G \left\{ \sum_{k \in \mathcal{K}_i} \left( \frac{\exp \left( \frac{1}{-\alpha} \frac{\bar{\mathbf{f}}^H \mathbf{A}_{c,\mathcal{K}_i}(k) \bar{\mathbf{f}}}{\bar{\mathbf{f}}^H \mathbf{B}_{c,\mathcal{K}_i}(k) \bar{\mathbf{f}}} \right)}{\sum_{j \in \mathcal{K}_i} \exp \left( \frac{1}{-\alpha} \log_2 \left( \frac{\bar{\mathbf{f}}^H \mathbf{A}_{c,\mathcal{K}_i}(j) \bar{\mathbf{f}}}{\bar{\mathbf{f}}^H \mathbf{B}_{c,\mathcal{K}_i}(j) \bar{\mathbf{f}}} \right) \right)} \right) \right\} \quad (79)$$

$$\times \left[ \frac{\mathbf{A}_{c,\mathcal{K}_i}(k) \bar{\mathbf{f}}}{\bar{\mathbf{f}}^H \mathbf{A}_{c,\mathcal{K}_i}(k) \bar{\mathbf{f}}} - \frac{\mathbf{B}_{c,\mathcal{K}_i}(k) \bar{\mathbf{f}}}{\bar{\mathbf{f}}^H \mathbf{B}_{c,\mathcal{K}_i}(k) \bar{\mathbf{f}}} \right] \quad (80)$$

$$+ \sum_{k=1}^K \left[ \frac{\mathbf{A}_k \bar{\mathbf{f}}}{\bar{\mathbf{f}}^H \mathbf{A}_k \bar{\mathbf{f}}} - \frac{\mathbf{B}_k \bar{\mathbf{f}}}{\bar{\mathbf{f}}^H \mathbf{B}_k \bar{\mathbf{f}}} \right] = 0. \quad (81)$$

If we properly define  $\mathbf{A}_{\text{KKT}}, \mathbf{B}_{\text{KKT}}$  as equation (54), (55), (56), we can arrange the first-order KKT condition as

$$\mathbf{A}_{\text{KKT}}(\bar{\mathbf{f}})\bar{\mathbf{f}} = \lambda(\bar{\mathbf{f}})\mathbf{B}_{\text{KKT}}(\bar{\mathbf{f}})\bar{\mathbf{f}} \Leftrightarrow \mathbf{B}_{\text{KKT}}(\bar{\mathbf{f}})^{-1}\mathbf{A}_{\text{KKT}}(\bar{\mathbf{f}})\bar{\mathbf{f}} \quad (82)$$

$$= \lambda(\bar{\mathbf{f}})\bar{\mathbf{f}}. \quad (83)$$

This completes the proof.

## REFERENCES

- [1] L. Lu, G. Y. Li, A. L. Swindlehurst, A. Ashikhmin, and R. Zhang, "An overview of massive MIMO: Benefits and challenges," *IEEE J. Sel. Topics Signal Process.*, vol. 8, no. 5, pp. 742–758, 2014.
- [2] T. L. Marzetta, "Noncooperative cellular wireless with unlimited numbers of base station antennas," *IEEE Trans. Wireless Commun.*, vol. 9, no. 11, pp. 3590–3600, 2010.
- [3] J. Flordelis, F. Rusek, F. Tufvesson, E. G. Larsson, and O. Edfors, "Massive MIMO performance—TDD versus FDD: What do measurements say?" *IEEE Trans. Wireless Commun.*, vol. 17, no. 4, pp. 2247–2261, 2018.
- [4] T. Choi, F. Rottenberg, J. Gómez-Ponce, A. Ramesh, P. Luo, C. J. Zhang, and A. F. Molisch, "Experimental investigation of frequency domain channel extrapolation in massive MIMO systems for zero-feedback FDD," *IEEE Trans. Wireless Commun.*, vol. 20, no. 1, pp. 710–725, 2021.
- [5] M. B. Khalilsarai, Y. Song, T. Yang, and G. Caire, "FDD massive MIMO channel training: Optimal rate-distortion bounds and the spectral efficiency of "One-Shot" schemes," *IEEE Trans. Wireless Commun.*, vol. 22, no. 9, pp. 6018–6032, 2023.
- [6] J. Jeon, G. Lee, A. A. Ibrahim, J. Yuan, G. Xu, J. Cho, E. Onggosanusi, Y. Kim, J. Lee, and J. C. Zhang, "MIMO evolution toward 6G: Modular massive MIMO in low-frequency bands," *IEEE Commun. Mag.*, vol. 59, no. 11, pp. 52–58, 2021.
- [7] J. Choi, D. J. Love, and T. Kim, "Trellis-extended codebooks and successive phase adjustment: A path from LTE-Advanced to FDD massive MIMO systems," *IEEE Trans. Wireless Commun.*, vol. 14, no. 4, pp. 2007–2016, 2015.
- [8] B. Lee, J. Choi, J.-Y. Seol, D. J. Love, and B. Shim, "Antenna grouping based feedback compression for FDD-based massive MIMO systems," *IEEE Trans. Commun.*, vol. 63, no. 9, pp. 3261–3274, 2015.
- [9] E. Zeydan, O. Dedeoglu, and Y. Turk, "Experimental evaluations of TDD-based massive MIMO deployment for mobile network operators," *IEEE Access*, vol. 8, pp. 33 202–33 214, 2020.
- [10] X. Rao and V. K. N. Lau, "Distributed compressive CSIT estimation and feedback for FDD multi-user massive MIMO systems," *IEEE Trans. Signal Process.*, vol. 62, no. 12, pp. 3261–3271, 2014.
- [11] Y. Han, J. Lee, and D. J. Love, "Compressed sensing-aided downlink channel training for FDD massive MIMO systems," *IEEE Trans. Commun.*, vol. 65, no. 7, pp. 2852–2862, 2017.
- [12] B. Wang, M. Jian, F. Gao, G. Y. Li, and H. Lin, "Beam squint and channel estimation for wideband mmWave massive MIMO-OFDM systems," *IEEE Trans. Signal Process.*, vol. 67, no. 23, pp. 5893–5908, 2019.
- [13] P. Liang, J. Fan, W. Shen, Z. Qin, and G. Y. Li, "Deep learning and compressive sensing-based CSI feedback in FDD massive MIMO systems," *IEEE Trans. Veh. Technol.*, vol. 69, no. 8, pp. 9217–9222, 2020.
- [14] Y. Yang, F. Gao, G. Y. Li, and M. Jian, "Deep learning-based downlink channel prediction for FDD massive MIMO system," *IEEE Commun. Lett.*, vol. 23, no. 11, pp. 1994–1998, 2019.
- [15] M. Alrabeiah and A. Alkhateeb, "Deep learning for TDD and FDD massive MIMO: Mapping channels in space and frequency," in *Proc. of Asilomar Conf. on Sign., Syst. and Computers*, 2019, pp. 1465–1470.
- [16] J. Guo, C.-K. Wen, S. Jin, and G. Y. Li, "Overview of deep learning-based CSI feedback in massive MIMO systems," *IEEE Trans. Commun.*, vol. 70, no. 12, pp. 8017–8045, 2022.
- [17] D. Vasisht, S. Kumar, H. Rahul, and D. Katabi, "Eliminating channel feedback in next-generation cellular networks," in *Proc. of the ACM SIGCOMM Conf.*, 2016, pp. 398–411.
- [18] F. Rottenberg, T. Choi, P. Luo, C. J. Zhang, and A. F. Molisch, "Performance analysis of channel extrapolation in FDD massive MIMO systems," *IEEE Trans. Wireless Commun.*, vol. 19, no. 4, pp. 2728–2741, Apr. 2020.
- [19] Z. Zhong, L. Fan, and S. Ge, "FDD massive MIMO uplink and downlink channel reciprocity properties: Full or partial reciprocity?" *Proc. IEEE Glob. Comm. Conf.*, Dec. 2020.
- [20] D. Han, J. Park, and N. Lee, "FDD massive MIMO without CSI feedback," *IEEE Trans. Wireless Commun.*, pp. 1–1, 2023.
- [21] Y. Han, T. H. Hsu, C. K. Wen, K. K. Wong, and S. Jin, "Efficient downlink channel reconstruction for FDD multi-antenna systems," *IEEE Trans. Wireless Commun.*, vol. 18, no. 6, pp. 3161–3176, June 2019.
- [22] M. A. Maddah-Ali and D. Tse, "Completely stale transmitter channel state information is still very useful," *IEEE Trans. Inf. Theory*, vol. 58, no. 7, pp. 4418–4431, 2012.
- [23] A. Adhikary, J. Nam, J.-Y. Ahn, and G. Caire, "Joint spatial division and multiplexing—the large-scale array regime," *IEEE Trans. Inf. Theory*, vol. 59, no. 10, pp. 6441–6463, 2013.
- [24] J. Park, B. Lee, J. Choi, H. Lee, N. Lee, S.-H. Park, K.-J. Lee, J. Choi, S. H. Chae, S.-W. Jeon, K. S. Kwak, B. Clerckx, and W. Shin, "Rate-splitting multiple access for 6G networks: Ten promising scenarios and applications," *IEEE Network*, pp. 1–1, 2023.
- [25] R. H. Etkin, D. N. C. Tse, and H. Wang, "Gaussian interference channel capacity to within one bit," *IEEE Trans. Inf. Theory*, vol. 54, no. 12, pp. 5534–5562, 2008.
- [26] H. Joudeh and B. Clerckx, "Sum-rate maximization for linearly precoded downlink multiuser MISO systems with partial CSIT: A rate-splitting approach," *IEEE Trans. Commun.*, vol. 64, no. 11, pp. 4847–4861, 2016.
- [27] Z. Li, C. Ye, Y. Cui, S. Yang, and S. Shamai, "Rate splitting for multi-antenna downlink: Precoder design and practical implementation," *IEEE J. Sel. Areas Commun.*, vol. 38, no. 8, pp. 1910–1924, 2020.
- [28] D. B. Amor, M. Joham, and W. Utschick, "Rate splitting in FDD massive MIMO systems based on the second order statistics of transmission channels," *IEEE J. Sel. Areas Commun.*, vol. 41, no. 5, pp. 1351–1365, May 2023.
- [29] J. Park, J. Choi, N. Lee, W. Shin, and H. V. Poor, "Rate-splitting multiple access for downlink MIMO: A generalized power iteration approach," *IEEE Trans. Wireless Commun.*, vol. 22, no. 3, pp. 1588–1603, Mar. 2023.
- [30] B. Efron and D. V. Hinkley, "Assessing the accuracy of the maximum likelihood estimator: Observed versus expected fisher information," *Biometrika*, vol. 65, no. 3, pp. 457–483, 1978.
- [31] B. G. Lindsay and B. Li, "On second-order optimality of the observed Fisher information," *The Annals of Statistics*, vol. 25, no. 5, pp. 2172–2199, 1997.
- [32] X. Cao and J. C. Spall, "Relative performance of expected and observed Fisher information in covariance estimation for maximum likelihood estimates," in *American Control Conference (ACC)*. IEEE, 2012, pp. 1871–1876.
- [33] M. Dai, B. Clerckx, D. Gesbert, and G. Caire, "A rate splitting strategy for massive MIMO with imperfect CSIT," *IEEE Trans. Wireless Commun.*, vol. 15, no. 7, pp. 4611–4624, 2016.
- [34] B. Clerckx, Y. Mao, E. A. Jorswieck, J. Yuan, D. J. Love, E. Erkip, and D. Niyato, "A primer on rate-splitting multiple access: Tutorial, myths, and frequently asked questions," *IEEE J. Sel. Areas Commun.*, 2023.
- [35] B. Mamandipoor, D. Ramasamy, and U. Madhoo, "Newtonized orthogonal matching pursuit: Frequency estimation over the continuum," *IEEE Trans. Signal Process.*, vol. 64, no. 19, pp. 5066–5081, Oct. 2016.
- [36] T. M. Kodinariya, P. R. Makwana *et al.*, "Review on determining number of cluster in k-means clustering," *International Journal*, vol. 1, no. 6, pp. 90–95, 2013.
- [37] E. Björnson, L. Sanguinetti, and M. Debbah, "Massive MIMO with imperfect channel covariance information," in *Proc. of Asilomar Conf. on Sign., Syst. and Computers*, 2016, pp. 974–978.
- [38] S. M. Kay, "Statistical signal processing: estimation theory," *Prentice Hall*, vol. 1, pp. Chapter–3, 1993.
- [39] J. Choi, N. Lee, S.-N. Hong, and G. Caire, "Joint user selection, power allocation, and precoding design with imperfect CSIT for multi-cell MU-MIMO downlink systems," *IEEE Trans. Wireless Commun.*, vol. 19, no. 1, pp. 162–176, 2020.
- [40] S. S. Christensen, R. Agarwal, E. De Carvalho, and J. M. Cioffi, "Weighted sum-rate maximization using weighted MMSE for MIMO-BC beamforming design," *IEEE Trans. Wireless Commun.*, vol. 7, no. 12, pp. 4792–4799, 2008.